doi:10.1093/plcell/koab062

THE PLANT CELL

THE PLANT CELL 2021: 33: 1771–1789

Research Article

The ubiquitin E3 ligase SR1 modulates the submergence response by degrading phosphorylated WRKY33 in *Arabidopsis*

Bao Liu [1,#], Yuanzhong Jiang [1,#], Hu Tang [1], Shaofei Tong [1], Shangling Lou [1], Chen Shao [1], Junlin Zhang [1], Yan Song [1], Ningning Chen [1], Hao Bi [1], Han Zhang [1], Junhua Li [2], Jianquan Liu [1] and Huanhuan Liu [1,*,†]

1 Key Laboratory for Bio-resources and Eco-environment & State Key Lab of Hydraulics & Mountain River Engineering, College of Life Sciences, Sichuan University, Chengdu 610065, China

2 College of Life Sciences, Henan Normal University, Xinxiang 453007, China

*Author for correspondence: liuhuanhuan85@163.com

†Senior author.

#These authors contributed equally to this work.

L.H.H. and L.B. designed the research. L.B., T.H., L.H.H., B.H., S.C., Z.J.L., C.N.N., T.S.F., L.S.L., S.Y., Z.H., and J.Y.Z. carried out the experiments. L.B. and J.Y.Z. analyzed the data. L.H.H. and L.B. wrote the manuscript, L.J.Q. and L.J.H. revised the article.

The author responsible for distribution of materials integral to the findings presented in this article in accordance with the policy described in the Instructions for Authors (https://academic.oup.com/plcell) is: Huanhuan Liu (liuhuanhuan85@163.com).

Abstract

Oxygen deprivation caused by flooding activates acclimation responses to stress and restricts plant growth. After experiencing flooding stress, plants must restore normal growth; however, which genes are dynamically and precisely controlled by flooding stress remains largely unknown. Here, we show that the *Arabidopsis thaliana* ubiquitin E3 ligase SUBMERGENCE RESISTANT1 (SR1) regulates the stability of the transcription factor WRKY33 to modulate the submergence response. SR1 physically interacts with WRKY33 in vivo and in vitro and controls its ubiquitination and proteasomal degradation. Both the *sr1* mutant and *WRKY33* overexpressors exhibited enhanced submergence tolerance and enhanced expression of hypoxia-responsive genes. Genetic experiments showed that *WRKY33* functions downstream of *SR1* during the submergence response. Submergence induced the phosphorylation of WRKY33, which enhanced the activation of *RAP2.2*, a positive regulator of hypoxia-response genes. Phosphorylated WRKY33 and RAP2.2 were degraded by SR1 and the N-degron pathway during reoxygenation, respectively. Taken together, our findings reveal that the on-and-off module SR1-WRKY33-*RAP2.2* is connected to the well-known N-degron pathway to regulate acclimation to submergence in *Arabidopsis*. These two different but related modulation cascades precisely balance submergence acclimation with normal plant growth.

Introduction

Hypoxia stress caused by waterlogging or flooding restricts plant growth and decreases both productivity and quality (Bailey-Serres et al., 2012a, 2012). Plants must develop strategies in order to adapt to flooding stress. Such adaptations include internode elongation and adventitious root formation (Hattori et al., 2009), petiole elongation (Bailey-Serres et al., 2012a, 2012b), and secondary aerenchyma development (Rhine et al., 2010). Gene expression and signal

Received December 23, 2020. Accepted February 08, 2021. Advance access publication February 22, 2021

transduction are also critical for plant survival under flooding stress. The plant hormone ethylene is a crucial early signal that initiates the flooding response (Sasidharan and Voesenek, 2015; Sasidharan et al., 2018). The second messengers nitric oxide (Igamberdiev and Hill, 2004; Zhan et al., 2018) and reactive oxygen species (ROS) (Yuan et al., 2017) further amplify this stress signal. Transcription factors (TFs) integrate these signals to activate hypoxia-related genes (Hinz et al., 2010; Gibbs et al., 2011; Licausi et al., 2011; Gasch et al., 2016; GiuntoLi et al., 2017; Gibbs and Holdsworth, 2020).

The group VII ethylene response factors (ERF-VIIs), with five members, are key TFs involved in the flooding response in *Arabidopsis thaliana* (Hinz et al., 2010; Gibbs et al., 2011; Licausi et al., 2011; GiuntoLi et al., 2017; Gibbs and Holdsworth, 2020). For instance, the ERF-VII TF RAP2.2 increases the expression of hypoxia-related genes (e.g. *ADH1* and *PDC1*) and enhances flooding tolerance (Hinz et al., 2010). These ERF-VII factors are subsequently oxidized, arginylated, and ubiquitinated to target them for proteolysis in order to turn off hypoxia responses by the N-degron pathway, which acts as a canonical oxygen sensing mechanism when plants are reoxygenating (Gibbs et al., 2011; Licausi et al., 2011; Gibbs and Holdsworth, 2020). Further knowledge is needed about how these ERF-VII TFs are regulated and how these regulatory mechanisms are modulated during reoxygenation.

During stress and subsequent recovery processes, TF proteins may directly bind to their target genes and positively or negatively regulate transcript expression via posttranslational modifications, that is, phosphorylation or ubiquitination (Orosa et al., 2018; Gui et al., 2019). For example, phosphorylated BASIC TRANSCRIPTION FACTOR3-LIKE protein positively regulates the expression of C-repeat-binding factors (CBFs) in *Arabidopsis*, further activating the expression of cold-response genes and enhancing freezing tolerance (Ding et al., 2018). These CBFs can also be negatively regulated by phosphorylated ICE1, which plays a major role in balancing the cold response and growth in plants (Li et al., 2017). Similarly, the E3 ligases DEHYDRATION-RESPONSIVE ELEMENT BINDING PROTEIN2A (DREB2A)-INTERACTING PROTEIN1 (DRIP1) and DRIP2 participate in plant drought stress responses by mediating the degradation of DREB2A (Qin et al., 2008), while the U-box type E3 ubiquitin ligases PUB25 and PUB26 positively regulate the cold stress response by negatively regulating MYB15 (Wang et al., 2019) in *Arabidopsis*.

Such ubiquitination is achieved by three types of enzymes: ubiquitin-activating enzyme (E1), ubiquitin-conjugating enzyme (E2), and E3 ubiquitin ligases. The ubiquitinated molecules attach to the target proteins, which are distinguished and recognized by the 26S proteasome for degradation (Sadanandom et al., 2012). Both phosphorylation and ubiquitination modifications of TF proteins may occur simultaneously during stress tolerance and recovery. For instance, phosphorylation of TF proteins may affect their susceptibility to E3 ligases for ubiquitination and degradation by the 26S proteasome (Spoel et al., 2009; Zhu et al., 2017; Min et al., 2019). This on-and-off regulatory process is widely involved in many aspects of diverse plant stress response (Stone et al., 2005; Min et al., 2019). However, how posttranslational modifications precisely and in a timely manner control flooding-response genes remains largely unknown, although the phosphorylation genes involved in this process, *MPK3*/*MPK6*, positively regulate the hypoxia response (Chang et al., 2012).

In this study, we reveal that the *Arabidopsis* protein SUBMERGENCE RESISTANT1 (SR1), an E3 ligase containing a REALLY INTERESTING GENE (RING)-HC type RING domain (Kosarev et al., 2002), negatively regulates the submergence response by degrading the phosphorylated TF WRKY33. The *sr1* mutant is resistant to submergence stress compared with the wild-type Columbia (Col), while introducing *pSR1:SR1* into *sr1* restored its submergence sensitivity. Experiments conducted both in vitro and in vivo confirmed that SR1 physically interacts with WRKY33 and modulates its stability. *WRKY33* functions genetically downstream of *SR1* in the submergence tolerance pathway. Furthermore, WRKY33, especially its phosphorylated form, activates *RAP2.2* directly to increase tolerance to submergence treatment. Finally, this submergence response is turned off via the degradation of phosphorylated WRKY33 by SR1 during the reoxygenation process. Overall, our study sheds light on the on-and-off process of submergence acclimation through phosphorylation and ubiquitination and provides valuable information for accelerating the breeding of flooding-resistant crops.

Results

SR1 negatively regulates submergence tolerance

To gain a better understanding of the role of E3 ligases in the submergence response, we examined homozygous T-DNA insertion mutants of a number of genes encoding putative ubiquitin E3 ligases with submergence stress-responsive expression (Supplemental Figure S1). One T-DNA mutant (SALK_076386) that carries a T-DNA insertion in the beginning of the last exon of *AT2G47090* and leads to fairly low expression of this gene (Supplemental Figure S2) was identified; this mutant showed enhanced submergence tolerance compared with wild-type plants (Figure 1A) and was named *sr1*. To confirm the negative role of *SR1* in submergence sensitivity, we performed genetic complementation by introducing *pSR1:SR1* into *sr1* plants (Supplemental Figure S3, C and D) and also obtained *35S:SR1* overexpressing plants (*SR1OE*) (Supplemental Figure 3, A and B). Phenotypic comparisons (Figure 1A), including measurements of survival rates (Figure 1B) and dry weights (DWs; Figure 1C), among Col, *sr1*, *pSR1:SR1*/*sr1*, and *SR1OE* plants after dark submergence (DS) treatment suggested that *SR1* is a negative regulator of submergence tolerance.

Next, we examined the role of *SR1* in oxidative stress responses during hypoxia. The plant membrane is damaged

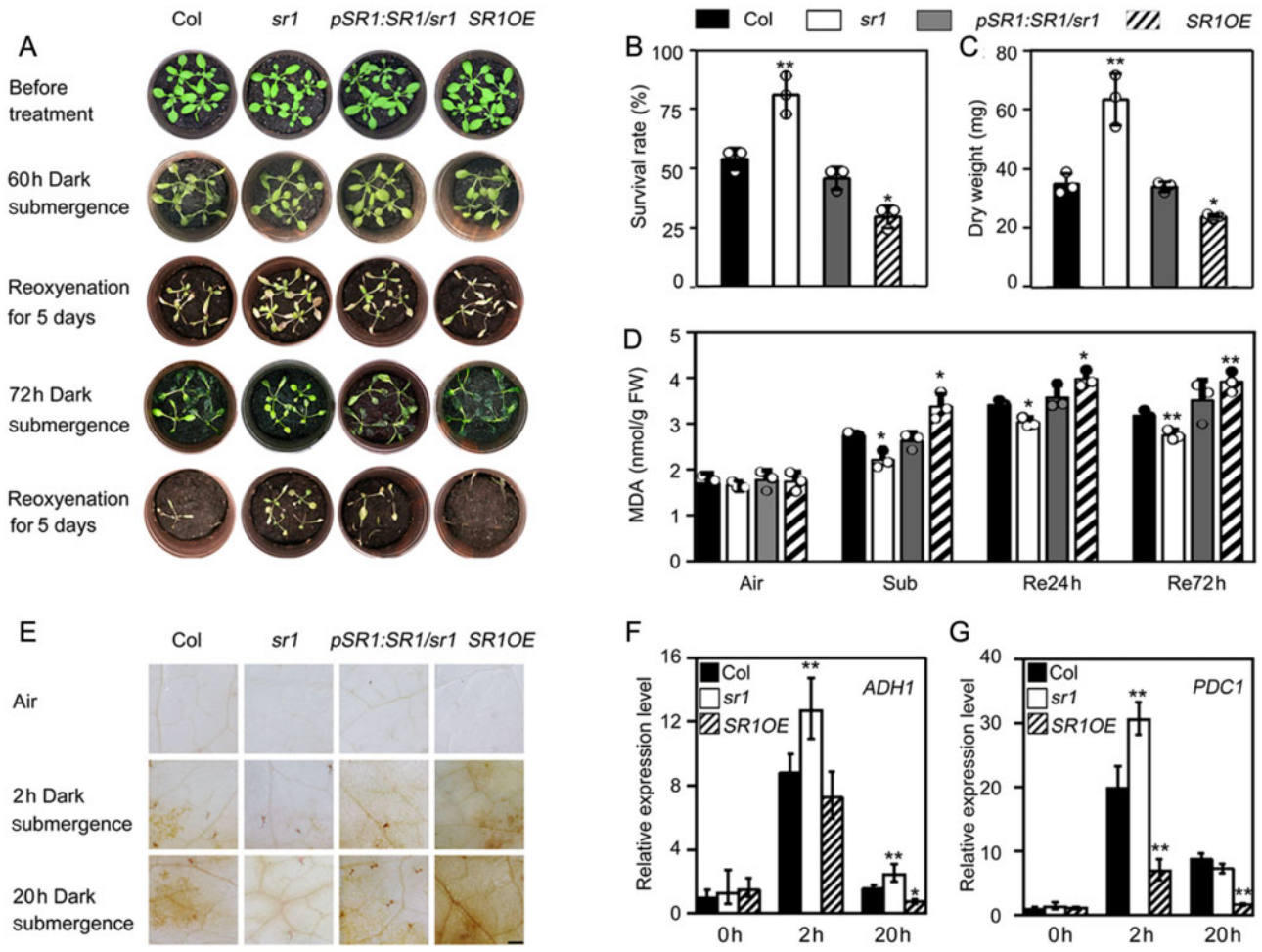

Figure 1 *SR1* negatively regulates the DS response in *Arabidopsis*. (A) Phenotypic analysis of Col, *sr1*, *pSR1:SR1/sr1*, and *SR1OE* plants treated with DS for 60 or 72 h, followed by 5 days of recovery. (B) Survival rates of Col, *sr1*, *pSR1:SR1/sr1*, and *SR1OE* plants treated with DS for 60 h, followed by 5 days of recovery. (C) DWs of Col, *sr1*, *pSR1:SR1/sr1*, and *SR1OE* plants treated with DS for 60 h, followed by 5 days of recovery and drying for 2 days. (D) MDA content of Col, *sr1*, *pSR1:SR1/sr1*, and *SR1OE* plants before submergence (Air) and after 2 days of DS (Sub) and subsequent recovery for 24 or 72 h. FW: fresh weight. (E) ROS accumulation detected by DAB staining in Col, *sr1*, *pSR1:SR1/sr1*, and *SR1OE* plants after treatment with or without DS for 2 or 20 h. Bar = 0.5 mm. (F–G) Total RNA was extracted from Col, *sr1*, and *SR1OE* plants treated by DS for the time periods indicated. *ADH1* and *PDC1* transcript levels were detected in Col, *sr1*, and *SR1OE* plants by qRT-PCR analysis. Data are average values ±SD (Standard Deviation) ($n = 3$) of three biological replicates (separate experiments). $^{**}P < 0.01$ and $^{*}P < 0.05$ indicate significant differences from Col.

by submergence stress, and malondialdehyde (MDA) is one of the main peroxidation products of membrane lipids; it can therefore be used to measure the degree of membrane damage. The content of ROS, especially hydrogen peroxide (H_2O_2), is another important indicator that reflects the extent to which plants are damaged during hypoxia stress induced by submergence. Excess ROS accumulation can injure plants. We, therefore, measured MDA contents (Figure 1D), H_2O_2 contents (by DAB staining; Figure 1E), ion leakage (Supplemental Figure S4A), and water loss rates (Supplemental Figure S4B) among the plants described above. The results support the conclusion that *SR1* negatively regulates submergence tolerance in *Arabidopsis*.

To further confirm the results of our submergence tolerance analysis, we examined the expression levels of several hypoxia-responsive marker genes in Col, *sr1*, and *SR1OE* plants during DS treatment. In response to 2 or 20 h of DS, the anaerobic respiration genes *ADH1* (Figure 1F), *PDC1* (Figure 1G), and *SUS4* (Supplemental Figure S5D); the hypoxia-responsive genes *PCO2*, *LBD41*, and *HB1* (Supplemental Figure S5, A–C), and the ethylene precursor biosynthetic gene *ACS2* (Supplemental Figure S5E) were all up-regulated in Col, *sr1* and *SR1OE* plants compared to the 0 h time point, indicating that the submergence treatment affected these plants. However, in most cases, the transcript levels of these genes were higher in *sr1* and to lower in *SR1OE* compared to wild-type plants in response to 2 and 20 h of submergence (Figure 1, F–G; Supplemental Figure S5). In some cases, the transcript levels were similar in WT and *SR1OE* plants, for example, *PCO2* at 2 h and *HB1* at 2 and 20 h (Figure 1, F–G; Supplemental Figure S5). The increased upregulation of these genes in the *sr1* mutant and

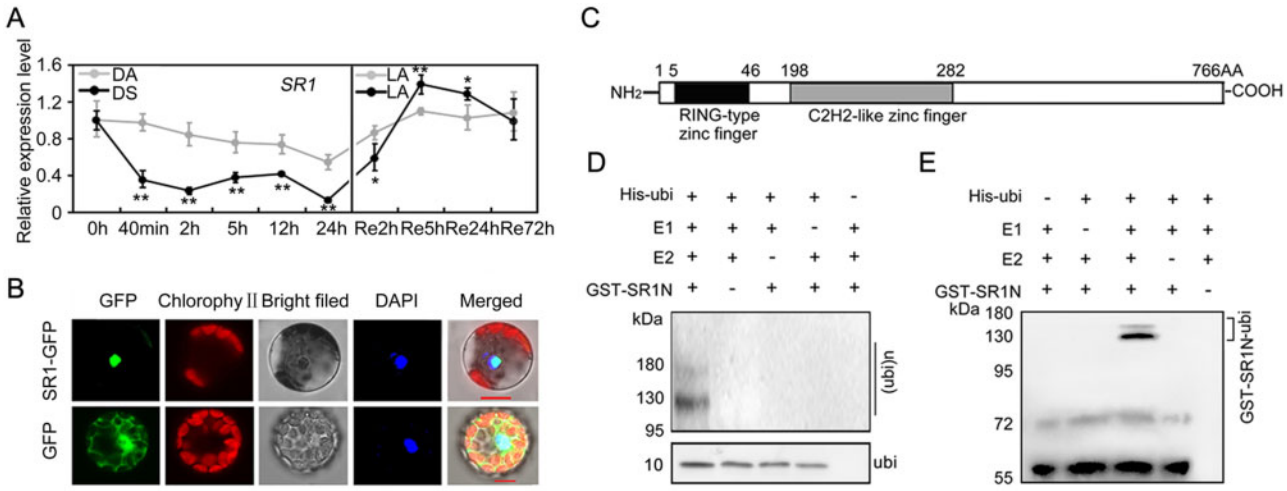

Figure 2 Expression profile of *SR1* and its ubiquitin E3 ligase activity. (A) qPCR analysis showing that *SR1* is repressed by DS but induced by reoxygenation compared with DA or LA treatment controls. Total RNA was extracted from Col and treated by submergence or reoxygenation (Re) after submergence for the time periods indicated. Three independent biological replicates were analyzed, and similar results were obtained. Data are average values ±SD ($n = 3$) of three biological replicates. $^{**}P < 0.01$ and $^{*}P < 0.05$ indicate significant differences from the control. (B) Subcellular localization analysis of SR1. *SR1-GFP* and *GFP* (control) constructs were transformed into *Arabidopsis* protoplasts. GFP fluorescence was detected under a laser-scanning confocal microscope. DAPI was used as a nuclear marker. At least 10 cells were observed, and they all showed similar expression patterns. Bars = 10 μm. (C) Schematic diagram showing the key domains (RING-type zinc finger and C2H2-like zinc finger) of SR1 protein. (D, E) Assays of in vitro self-ubiquitination of SR1. "+" and "-" denote the presence or absence of the components of each reaction mixture. The molecular weight of GST-SR1N is ~62 kDa. Protein ubiquitination bands generated by GST-SR1N are indicated on the right, and protein molecular mass markers are labeled on the left. Anti:HIS (D) and anti:GST (E) antibodies were used for immunoblot analysis. The band at 72 kDa (E) is an unspecific band.

reduced upregulation in *SR1OE* plants appears to be associated with their submergence resistant and hypersensitive phenotypes, respectively.

SR1 Is repressed by submergence and encodes a ubiquitin E3 ligase

Having shown that *SR1* plays a negative role in the submergence response, we examined the detailed timeline of *SR1* expression during DS treatment and the reoxygenation process. As shown in Figure 2A, *SR1* expression was repressed by DS treatment, which peaked at 24 h after treatment, while it was gradually up-regulated during reoxygenation, hinting at a possible role for *SR1* in this process. Notably, since a homolog of *SR1* (which we named *SR1 HOMOLOGOUS GENE1* (*SRH1*) (*AT3G62240*)) is present in *Arabidopsis* (Supplemental Figure S6A), we also examined the expression pattern of *SRH1* upon DS treatment. As shown in Supplemental Figure S6B, *SRH1* expression was not induced or repressed by DS treatment or during the reoxygenation process compared to the dark air (DA) control (grown in the dark without submergence), indicating that *SR1H* is not regulated in a similar manner to *SR1* during submergence and reoxygenation.

We generated a construct consisting of the *GUS* gene driven by a 1kb fragment of the *SR1* promoter and introduced it into the *Arabidopsis* Col ecotype to further study the expression pattern of *SR1* under hypoxia. Hypoxic conditions (1% oxygen) were achieved by constantly bubbling 99.999% nitrogen into the culture chamber for 12 h. Weak GUS staining was observed mainly in the shoot, whereas the root still showed substantial GUS staining. However, weak GUS staining was detected after hypoxia treatment (Supplemental Figure S7), supporting our observation that *SR1* was repressed by hypoxia resulting from submergence treatment (Figure 2A).

A subcellular localization experiment showed that SR1 co-localized with the nuclear dye DAPI and is therefore localized to the nucleus (Figure 2B), hinting at a possible role for the putative E3 ligase SR1 in regulating protein stability in the nucleus. We also investigated the expression patterns of *SR1* in different tissues. *SR1* was constitutively expressed in all tissues examined, including roots, shoots, rosette leaves, flowers, and fruit pods (Supplemental Figure S8). *SR1* encodes a 766 amino acid (AA) protein that contains a RING-HC type RING domain (Kosarev et al., 2002) near the N-terminal region (Figure 2C), suggesting that it likely has E3 ligase activity (Kraft et al., 2005; Stone et al., 2005). We, therefore, performed in vitro ubiquitination assays using purified SR1 protein. A GST-fusion protein (with 383 AAs from the N-terminal region of SR1 containing the RING domain) was purified, because we failed to obtain the full-length SR1 fusion protein. The GST-SR1N383 protein (GST-SR1N) was incubated with E1, E2, and His-ubiquitin (His-ubi) proteins, and the reaction products were analyzed by immunoblotting using anti-His and anti-GST antibodies (Figure 2, D and E). The formation of at least two high molecular mass bands was detected only when all reaction components were added, whereas reactions lacking any one of the components

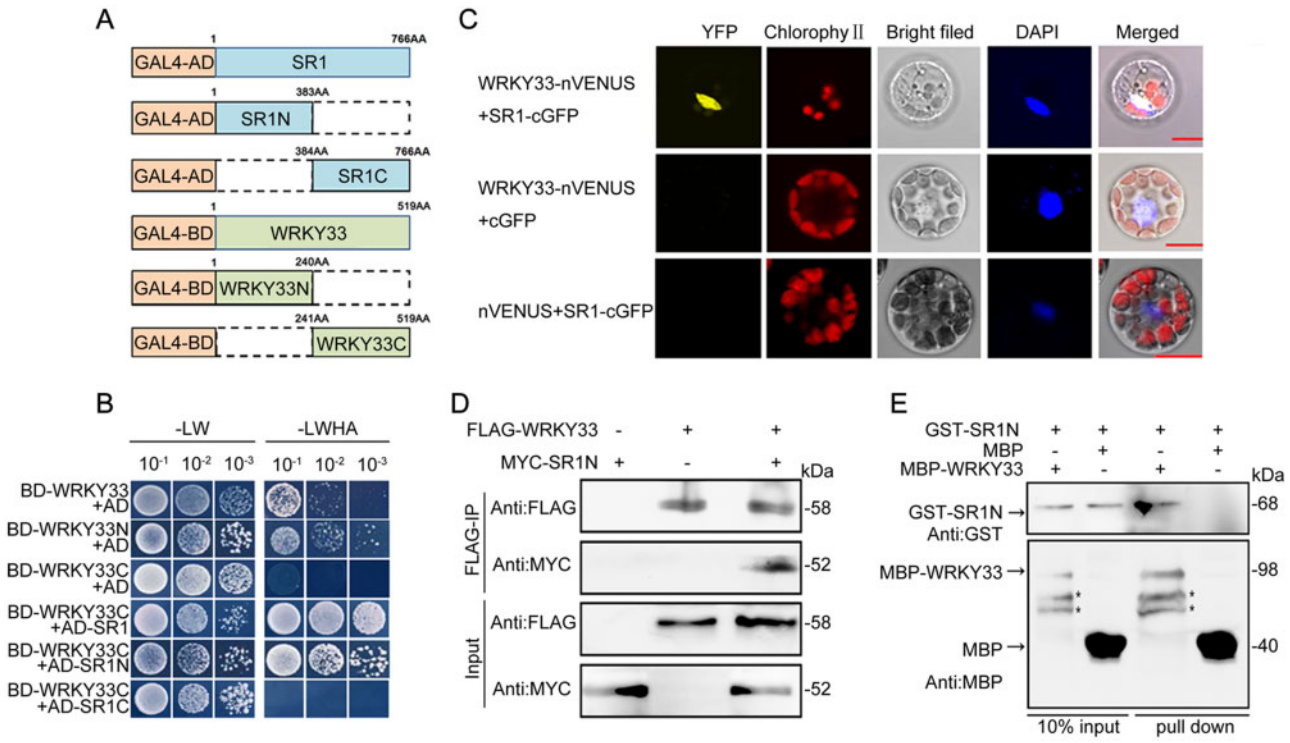

Figure 3 SR1 interacts with WRKY33 both in vivo and in vitro. (A) Schematic diagram showing the various constructs used in the Y2H analysis. Different numbers indicate the full-length or truncated SR1 and WRKY33 proteins. (B) Y2H analysis of the interaction between SR1 and WRKY33. The full-length SR1 protein and its C-terminal and N-terminal regions were each fused with the GAL4-transcription AD. The full-length WRKY33 protein and its C-terminal and N-terminal regions were each fused with the GAL4-DNA BD. Transformants were plated on synthetic dropout (SD) medium without leucine or tryptophan (-LW) and transferred to SD medium without leucine, tryptophan, histidine, or alanine (-LWHA) to detect interactions. Here, 10^{-1}, 10^{-2}, and 10^{-3} indicate dilution concentrations of 10, 100, and 1000 times, respectively. (C) BiFC assay of the interaction between SR1 and WRKY33. WRKY33-nVENUS and SR1-cGFP or WRKY33-nVENUS and cCFP or SR1-cGFP and nVENUS constructs were co-transformed into *Arabidopsis* protoplasts to detect the interaction between SR1 and WRKY33 in vivo. YFP fluorescence was detected under a laser-scanning confocal microscope. At least 10 cells were observed, and similar results were obtained. Bars = 10 μm. (D) Co-IP to examine the interaction between SR1 and WRKY33. Proteins were isolated from *N. benthamiana* leaves expressing *35S:MYC-SR1N* and *35S:FLAG-WRKY33* for 3 days. Anti:FLAG beads were used for the IP experiment. Anti:MYC and anti:FLAG antibodies were used for immunoblot analysis. (E) In vitro pull-down assay to examine the interaction between SR1 and WRKY33. Purified proteins (GST-SR1N, MBP-WRKY33, and MBP) were used. MBP affinity beads were used for the pull-down assay. Anti:MBP and anti:GST antibodies.

E1, E2, His-ubi, or GST-SR1N failed to produce a positive result (Figure 2, D and E). These results demonstrate that SR1 functions as a RING-type E3 ligase in vitro and can mediate self-ubiquitination and form a polyubiquitinated chain.

SR1 physically interacts with WRKY33 both in vivo and in vitro

We thus far demonstrated that SR1 participates in the submergence-induced hypoxia response and functions as an E3 ligase. E3 ligases commonly facilitate protein degradation via physical interactions with their target substrate proteins. We, therefore, looked for targets of SR1 during the submergence process. We performed Yeast two-hybrid (Y2H) screening using the full-length SR1 protein fused with GAL4-BD as a bait and screened a cDNA library constructed from 24 h-dark-submergence-treated leaves of 2-week-old Col plants. WRKY33, a key factor in biotic and abiotic defense pathways (Zheng et al., 2006; Lai et al., 2011; Liu et al., 2015; Liao et al., 2016), was identified as a putative partner of SR1. To validate their interaction, we fused full-length SR1, 383 AAs of the N-terminus (SR1N), and 383 AAs of the C-terminus of SR1 (SR1C) to the activation domain (AD) of GAL4 and full-length WRKY33, 240 AAs of the N-terminus (WRKY33N), and 279 AAs of the C-terminus of WRKY33 (WRKY33C) to the DNA binding domain (BD) of GAL4 (Figure 3A) to examine the interaction between SR1 and WRKY33. A Y2H experiment showed that WRKY33N had self-activation activity whereas WRKY33C did not. Meanwhile, SR1 interacted with the C-terminal region (279 AAs) of WRKY33 (WRKY33C), and WRKY33C interacted with the N-terminal region of SR1 including 383 AAs containing the RING domain (SR1N) (Figure 3B).

We also examined this interaction by performing a Y2H assay between the product of the homologous gene *SRH1* and WRKY33. These two proteins failed to interact with each other (Supplemental Figure S9), pointing to functional differentiation between *SR1* and its homolog *SRH1* (*AT3G62240*). We performed bimolecular fluorescence

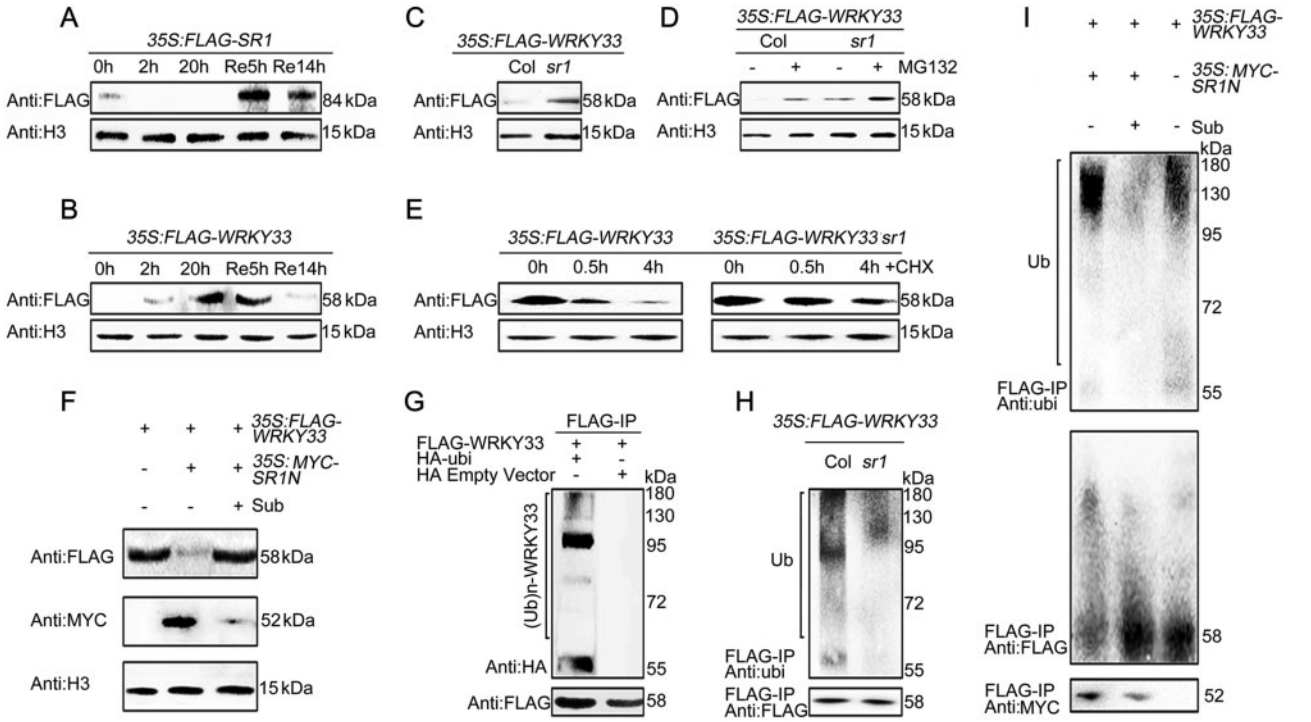

Figure 4 SR1 Promotes the degradation of WRKY33. (A) Nuclear protein levels of SR1 examined using *35S:FLAG-SR1* plants subjected to dark submergence treatment and during the reoxygenation process for the time periods indicated. (B) Nuclear protein levels of WRKY33 examined using *35S:FLAG-WRKY33* plants subjected to dark submergence treatment and during the reoxygenation process for the time periods indicated. (C) Nuclear protein levels of WRKY33 examined in *35S:FLAG-WRKY33* and *35S:FLAG-WRKY33 sr1* plants. (D) Effects of MG132, a chemical inhibitor of the 26S proteasome, on the stability of WRKY33. WRKY33 protein levels were examined in *35S:FLAG-WRKY33* and *35S:FLAG-WRKY33 sr1* plants supplied with or without 50 μM MG132 for 24 h. (E) WRKY33 showed a decrease in turnover rate in *sr1* compared to Col plants. Two-week-old *35S:FLAG-WRKY33* and *35S:FLAG-WRKY33 sr1* plants were treated with 100 mM CHX for the time periods indicated. Nuclear proteins were isolated and analyzed by immunoblotting. (F) Nuclear proteins were isolated from *N. benthamiana* leaves after expressing *35S:FLAG-WRKY33* alone, or *35S:FLAG-WRKY33* and *35S:MYC-SR1N* together for 3 days following 20 h dark submergence treatment or control treatment (dark air was used as the control(-)). Anti:FLAG and anti:MYC antibodies were used for detection. (A–F) Nuclear proteins were extracted from rosette leaves of 3-week-old transgenic plants and histone H3 was used as the internal control. The molecular weight of FLAG-SR1 is 84 kDa, FLAG-WRKY33 is 58 kDa and MYC-SR1N is 52 kDa. (G) Levels of WRKY33 ubiquitination detected in vivo by an IP experiment. *N. benthamiana* leaves after expressing *35S:FLAG-WRKY33* and HA empty vector or *35S:FLAG-WRKY33* and 35S:HA-ubi for 3 days were used for the IP experiment. Anti:HA and anti:FLAG antibodies were used for immunoblot analysis. The empty HA vector was used as a negative control. Protein molecular mass markers are labeled on the right. (H) Levels of WRKY33 ubiquitination detected in *35S:FLAG-WRKY33* and *35S:FLAG-WRKY33 sr1* plants. Nuclear proteins were isolated from rosette leaves of 3-week-old *35S:FLAG-WRKY33* and *35S:FLAG-WRKY33 sr1* plants followed by a FLAG-IP experiment. The levels of *FLAG-WRKY33* ubiquitination were examined using an anti:ubi antibody. (I) Nuclear proteins were isolated from *N. benthamiana* leaves after expressing *35S:FLAG-WRKY33* without treatment, or expressing *35S:FLAG-WRKY33* and *35S:MYC-SR1N* together and carrying out a 20 h dark submergence treatment or control treatment (dark air was used as the control(-)), and used in a FLAG-IP experiment. The levels of FLAG-WRKY33 ubiquitination were examined using an anti:ubi antibody.

complementation (BiFC), Co-immunoprecipitation (IP) and pull-down experiments to further validate the interaction between SR1 and WRKY33. As shown in Figure 3C, SR1 interacted with WRKY33 in the nucleus in the BiFC experiment. The Co-IP experiment showed that SR1N interacts with WRKY33 in vivo (Figure 3D). The pull-down experiment using MBP-affinity beads showed that GST-SR1N interacts with MBP-WRKY33 in vitro (Figure 3E).

SR1 ubiquitinates WRKY33 and facilitates its degradation

The physical interaction between SR1 and WRKY33 led us to examine whether SR1 can ubiquitinate WRKY33 for degradation during the reoxygenation process after submergence treatment. First, we examined their expression patterns during DS treatment and during reoxygenation using transgenic lines overexpressing *35S:FLAG-SR1* (Supplemental Figure S10) and *35S:FLAG-WRKY33* (*WRKY33OE*) (Supplemental Figure S11) in the Col background. As shown in Figure 4, A and B, the level of SR1 decreased upon DS and increased during the reoxygenation process. By contrast, the level of WRKY33 increased upon DS and declined during reoxygenation. To determine whether the changes in protein levels were caused by changes in mRNA expression, we examined the mRNA levels of *FLAG-SR1* and *FLAG-WRKY33* upon DS treatment. The expression of these genes was not affected by this treatment (Supplemental Figure S12). The repressed expression of *SR1*

mRNA (Figure 2A) and SR1 protein (Figure 4A) upon DS treatment suggested that DS might lead to both downregulation of *SR1* at the mRNA level and a concomitant increase in protein degradation.

To investigate this notion, we examined the SR1 level upon DS in the presence or absence of MG132, a chemical inhibitor of the 26S proteasome. As shown in Supplemental Figure S13, MG132 treatment indeed prevented the degradation of SR1 during DS, confirming our hypothesis. The opposite expression patterns were observed during the submergence treatment and reoxygenation, suggesting that SR1 might mediate the degradation of WRKY33 during these processes. To further confirm this notion, we obtained *35S:FLAG-WRKY33 sr1* plants by genetic crossing. To exclude the possibility of gene silencing during crossing, we examined the transcript levels of *FLAG-WRKY33*. *FLAG-WRKY33* transcript levels were similar in *35S:FLAG-WRKY33* and *35S:FLAG-WRKY33 sr1* plants (Supplemental Figure S14).

We also examined WRKY33 protein levels in *35S:FLAG-WRKY33* and *35S:FLAG-WRKY33 sr1* plants by immunoblot analysis. WRKY33 abundance was considerably elevated in rosette leaves of *35S:FLAG-WRKY33 sr1* plants compared to *35S:FLAG-WRKY33* plants (Figure 4C). To confirm that the degradation of WRKY33 is mediated by SR1 via the 26S proteasome, we examined the effect of MG132 on the stability of WRKY33. Immunoblot analysis showed that WRKY33 abundance was considerably elevated upon MG132 treatment (Figure 4D), suggesting that the 26S proteasome pathway modulates WRKY33 homeostasis. To further test the stability of WRKY33, we employed cycloheximide (CHX) to block new protein synthesis. WRKY33 showed a decreased turnover rate in the *sr1* mutant compared to Col plants (Figure 4E).

We performed transient expression in *Nicotiana benthamiana* leaves to test the possibility that WRKY33 levels are modulated by SR1. The expression of WRKY33 was clearly repressed when *35S:FLAG-WRKY33* and *35S:MYC-SR1N* were co-expressed compared to the expression of *35S:FLAG-WRKY33* alone in *N. benthamiana* leaves, while this was blocked by 20 h DS treatment, which inhibited the expression of SR1N protein (Figure 4F; Supplemental Figure S15). Collectively, these results suggest that SR1 mediates the degradation of WRKY33, likely via the 26S proteasome pathway. Interestingly, the WRKY33 level was also elevated in the *sr1* background (Figure 4D), suggesting that WRKY33 is not targeted for degradation solely by SR1.

To further confirm that SR1 can ubiquitinate WRKY33 and facilitate its degradation, we performed IP experiments. *35S:FLAG-WRKY33*, *35S:HA-ubi* as well as *35S:FLAG-WRKY33* and the control vector *35S:HA* were co-expressed in *N. benthamiana* leaves. IP was carried out using the anti-FLAG antibody conjugated agarose beads. Ubiquitinated WRKY33 proteins were detected as expected (Figure 4G). To examine whether the ubiquitination of WRKY33 is mediated via SR1, we performed another IP experiment in rosette leaves among *35S:FLAG-WRKY33* and *35S:FLAG-WRKY33 sr1* plants, again using anti-FLAG antibody conjugated agarose beads. Immunoblot analysis showed that knocking out *SR1* partially blocked the ubiquitination of WRKY33 (Figure 4H), suggesting that the ubiquitination of WRKY33 occurs via SR1. We also examined whether submergence treatment would affect the ubiquitination of WRKY33. *35S:FLAG-WRKY33* and *35S:MYC-SR1N* were co-expressed in *N. benthamiana* leaves for 3 days, followed by 20 h of DS vs. the control. A FLAG-IP experiment showed that the ubiquitination of WRKY33 was greatly weakened under DS (Figure 4I), perhaps due to a decrease in mRNA levels as well as the destabilization of SR1 protein under these conditions. Taken together, these results suggest that submergence suppresses SR1 via an unknown mechanism, but promotes WRKY33 accumulation by suppressing 26S proteasome mediated, ubiquitin-associated degradation via SR1. Thus, we confirmed that WRKY33 is a target of the E3 ligase SR1 and can be degraded by SR1 via 26S proteasome-mediated degradation.

WRKY33 positively regulates the submergence response and is epistatic to *SR1*

Having confirmed that *SR1* negatively regulates the submergence response in *Arabidopsis* and that WRKY33 is a direct target of SR1, we hypothesized that WRKY33 might also participate in the submergence response together with SR1. To validate this notion, we obtained a *wrky33* mutant (SALK_006603) (Liao et al., 2016) and *WRKY33* overexpressing lines (*WRKY33OE*). Phenotypic analysis showed that *WRKY33OE* plants were more tolerant, while *wrky33* mutant was hypersensitive, to DS compared to the wild-type (Supplemental Figure S16A). Further experiments measuring survival rates (Supplemental Figure S16B), DWs (Supplemental Figure S16C), MDA contents (Supplemental Figure S16D), ion leakage (Supplemental Figure S16E), and water loss (Supplemental Figure S16F) all confirmed that *WRKY33* is a positive regulator of the submergence response.

We examined the expression of several hypoxia-responsive marker genes in Col, *wrky33*, and *WRKY33OE* plants upon DS treatment by qRT-PCR (Quantitative Reverse Transcription-PCR). The expression of genes related to anaerobic respiration, including *ADH1*, *PDC1*, and *SUS4* (Supplemental Figure S17), was repressed in the *wrky33* mutant and activated in *WRKY33OE* plants in response to 2 or 20 h of DS treatment. Other hypoxia-responsive marker genes, such as *PCO2* and *HB1*, as well as the ethylene biosynthesis gene *ACS2*, showed similar expression patterns (Supplemental Figure S17). The downregulation of these genes in the *wrky33* mutant and upregulation in *WRKY33OE* plants appeared to be associated with their respective submergence hypersensitive and resistant phenotypes. Different *WRKY33OE* transgenic lines were used in this work compared to our recent study (Tang et al., 2020), while similar results were obtained, further confirming the notion that *WRKY33* is a positive regulator of the submergence response.

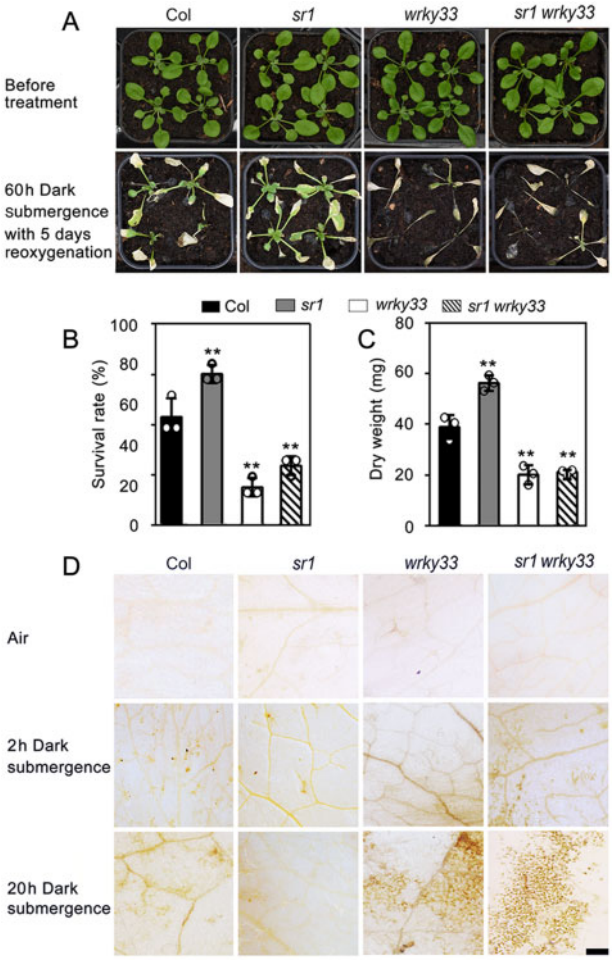

Figure 5 *WRKY33* functions downstream of *SR1* to positively regulate the dark submergence response in *Arabidopsis*. (A) Phenotypic analysis of Col, *sr1*, *wrky33*, and *sr1 wrky33* plants treated with dark submergence for 60 h, followed by 5 days of recovery. (B) Survival rates of Col, *sr1*, *wrky33*, and *sr1 wrky33* plants treated with dark submergence for 60 h, followed by 5 days of recovery. (C) DWs of Col, *sr1*, *wrky33*, and *sr1 wrky33* plants treated with dark submergence for 60 h, followed by 5 days of recovery and drying for 2 days. (D) ROS accumulation detected in Col, *sr1*, *wrky33*, and *sr1 wrky33* plants by DAB staining after treatment with or without dark submergence for 2 or 20 h. Bar = 0.5 mm. Data are average values ±SD (n = 3) of three independent biological replicates. **$P < 0.01$ indicates significant differences from Col.

To confirm the genetic hierarchy between *SR1* and *WRKY33*, we crossed the *sr1* mutant with the *wrky33* mutant. As shown in Figure 5A, the *sr1* mutant is tolerant to DS, whereas *wrky33* exhibited enhanced sensitivity to this treatment compared to the wild-type. The appearance of the double mutant *sr1 wrky33* was comparable to that of *wrky33*, and it also exhibited enhanced sensitivity to DS treatment (Figure 5A). Further experiments, including survival rate (Figure 5B), DW (Figure 5C), and DAB staining (Figure 5D) analyses also confirmed that *sr1 wrky33* showed enhanced sensitivity to DS treatment. We then examined the expression of the anaerobic respiration genes *ADH1* and *PDC1* by qRT-PCR . The expression of both genes was repressed in *sr1 wrky33* plants upon 2 or 20-h DS treatment (Supplemental Figure S18), as also observed for *wrky33* (Supplemental Figure S18). All of these experiments provide further evidence that *WRKY33* functions downstream of *SR1* and that they act in the same genetic pathway to participate in the submergence response.

WRKY33 directly activates *RAP2.2* to participate in the submergence response

WRKY33, a WRKY family protein containing a WRKY domain, regulates the expression of downstream genes via its W box element (Mao et al., 2011). To further explore the molecular mechanism underlying the role of WRKY33 in the submergence response, we screened for possible downstream target genes of WRKY33 by qRT-PCR. ERF-VII family genes are key regulators of the submergence response (Hinz et al., 2010; Gibbs et al., 2011; Licausi et al., 2011; GiuntoLi et al., 2017; Gibbs and Holdsworth, 2020). The promoters of four members (*RAP2.2*, *RAP2.12*, *HRE1*, and *HRE2*) of the ERF-VII family contain a W box *cis*-element, which is a putative binding site for WRKY33. We performed qRT-PCR to examine the expression patterns of these four genes in Col, *wrky33*, and *WRKY33OE* plants during DS. Only *RAP2.2* transcript levels were positively correlated with the expression levels of *WRKY33* upon 2 or 20 h DS treatment (Supplemental Figure S19), suggesting that WRKY33 might

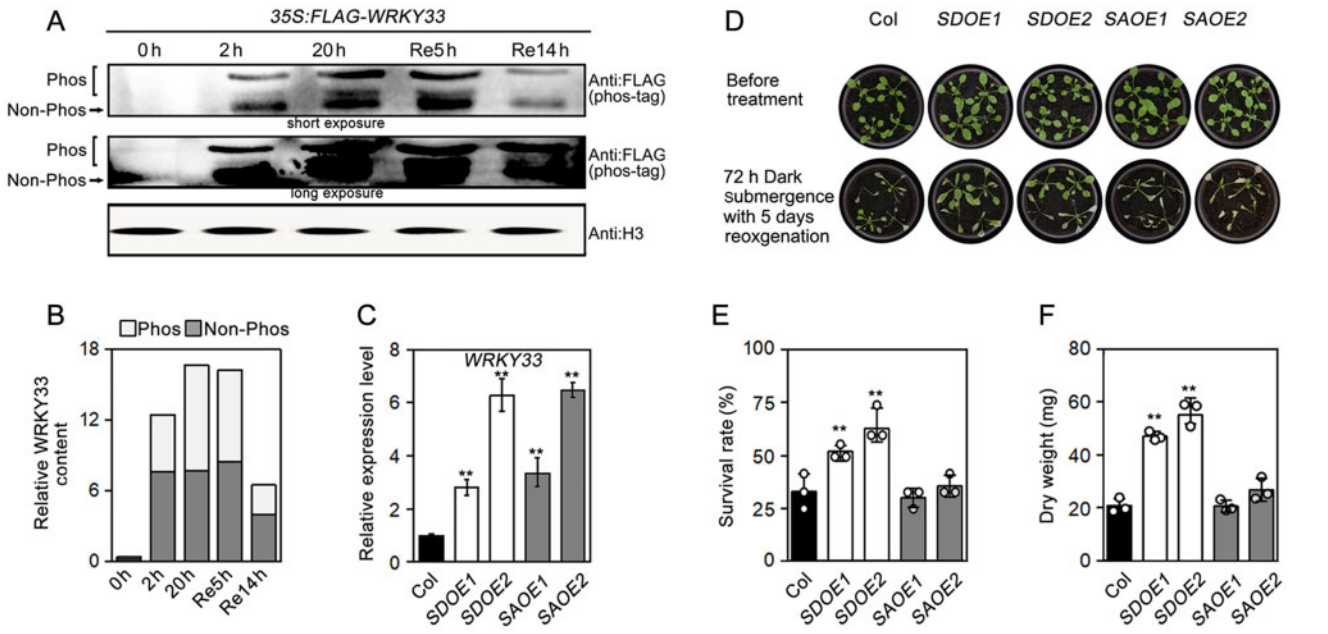

Figure 6 SD but Not SA overexpression enhances tolerance to dark submergence. (A) Dark submergence treatment induces the accumulation of phosphorylated WRKY33, while reoxygenation removes it (top panel shows a short exposure, middle panel shows a long exposure). Phosphorylated and non-phosphorylated WRKY33 proteins were separated using a phos-tag gel. Histone H3 was used as the internal nuclear protein loading control. The molecular weight of FLAG-WRKY33 is 58 kDa, H3 is 15 kDa. (B) Phosphorylated and non-phosphorylated WRKY33 proteins quantified using ImageJ software with the value for the first lane set as 1. The middle panel (long exposure) in Figure 6A was used to quantify protein levels. (C) *WRKY33* expression levels in *SDOE1*, *SDOE2*, *SAOE1*, and *SAOE2* plants are determined by qPCR. Total RNA was extracted from 3-week-old *SDOE1*, *SDOE2*, *SAOE1*, and *SAOE2* plants. (D) Phenotypic analysis of Col, *SDOE1*, *SDOE2*, *SAOE1*, and *SAOE2* plants after dark submergence treatment for 72 h, followed by 5 days of recovery. (E) Survival rates of Col, *SDOE1*, *SDOE2*, *SAOE1*, and *SAOE2* plants determined after dark submergence treatment for 72 h, followed by 5 days of recovery. (F) DWs of Col, *SDOE1*, *SDOE2*, *SAOE1*, and *SAOE2* plants measured after dark submergence treatment for 72 h, followed by 5 days of recovery and drying for 2 days. Data are average values ±SD ($n = 3$) of independent biological replicates. $^{**}P < 0.01$ indicates significant differences from Col.

positively regulate *RAP2.2* expression. Furthermore, we examined the expression of *RAP2.2*, *RAP2.12*, *HRE1*, and *HRE2* in Col, *sr1*, and *SR1OE* plants treated with DS and again, only *RAP2.2* transcript levels were elevated (Supplemental Figure S20) in the *sr1* mutant, which showed an increase in WRKY33 protein levels (Figure 4C). The *RAP2.2* transcript level in the *sr1 wrky33* double mutant was comparable to that in the *wrky33* mutant (Supplemental Figure S21), suggesting that *RAP2.2* might be regulated by *WRKY33*. We also analyzed the expression patterns of *WRKY33* and *RAP2.2* in response to submergence treatment and the reoxygenation process. *WRKY33* expression was induced at 20 min, whereas *RAP2.2* expression was not induced until 40 min upon submergence treatment (Supplemental Figure S22), again pointing to the possible regulation of *RAP2.2* by WRKY33.

To further confirm that WRKY33 directly regulates *RAP2.2*, we performed ChIP-qPCR experiments using *WRKY33OE* plants under normal and DS conditions. WRKY33 directly bound to the P2 fragment containing a W box in the promoter of *RAP2.2* in vivo under normal conditions (Supplemental Figure S23, A–C). Interestingly, a 20 h-dark-submergence treatment clearly increased the binding of WRKY33 to the P2 fragment of *RAP2.2* (Supplemental Figure S23D), suggesting that the stabilization and accumulation of WRKY33 were induced by submergence treatment (Supplemental Figure S23B). In an Electrophoretic Mobility Shift Assay (EMSA), purified MBP-WRKY33 protein directly bound to the W box in the *RAP2.2* promoter, but the mutant probe did not (Supplemental Figure S23F). MBP alone did not bind to the probe (Supplemental Figure S23E). In a dual-luciferase experiment, WRKY33 activated the expression of *RAP2.2* in vivo, whereas mutating the W box or adding SR1 protein blocked this activation (Supplemental Figure S23, G–I). Taken together, these results indicate that *RAP2.2* is directly up-regulated by WRKY33 via its W-box element.

To confirm the genetic hierarchy of *RAP2.2* and *WRKY33*, we obtained *35S:RAP2.2* (*RAP2.2OE*) plants and crossed them with the *wrky33* mutant (Supplemental Figure S24A). As shown in Supplemental Figure S24B, overexpressing *RAP2.2* in the *wrky33* background rescued the submergence hypersensitive phenotype of *wrky33*, which was also verified by survival rate (Supplemental Figure S24C) and DW measurements (Supplemental Figure S24D). In brief, these findings suggest that *RAP2.2* functions downstream of *WRKY33* and that they act in the same genetic pathway to control the submergence response of *Arabidopsis*.

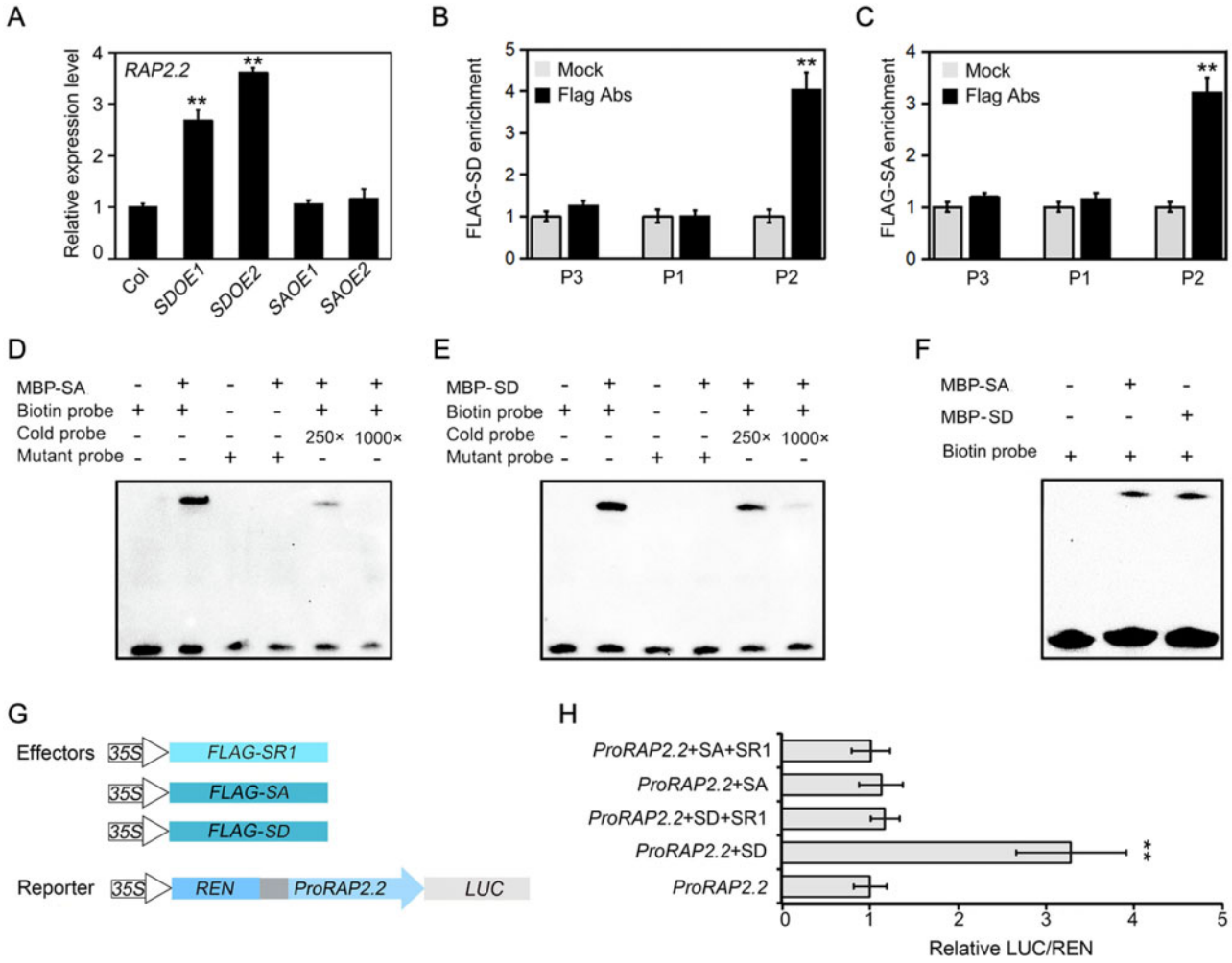

Figure 7 SD but not SA induces *RAP2.2* expression. (A) qPCR analysis showing *RAP2.2* expression levels in Col, *SDOE1*, *SDOE2*, *SAOE1*, and *SAOE2* plants. (B, C) ChIP-qPCR analysis showing that the binding ability of FLAG-SD to the *RAP2.2* promoter is comparable to that of FLAG-SA in vivo. DNA/protein complexes were isolated from *35S:FLAG-WRKY33SD/SA* transgenic plants line2#. Relative enrichment of *RAP2.2* promoter was determined by qPCR and calculated against input levels. (D, E) The abilities of MBP-SD and MBP-SA to bind to the promoter of *RAP2.2* examined by EMSA. Here 250× and 1000× cold probes were used as competitors. (F) Comparison of the binding ability of MBP-SD and MBP-SA to the *RAP2.2* promoter by EMSA. Equal amounts of MBP-SD and MBP-SA proteins were used. (D–F) 12% native gels were used to separate the free or bound DNA-protein complexes. (G) Schematic diagram of effectors (including *35S:FLAG-SR1*, *35S:FLAG-SA*, *35S:FLAG-SD*) and reporter (*proRAP2.2:LUC*). (H) The reporter *proRAP2.2:LUC* together with the indicated effectors was co-infiltrated into *N. benthamiana* leaves and expressed for 3 days. LUC and REN values were then measured. The value for *proRAP2.2:LUC* was set to 1.0. Data are average values ±SD ($n = 3$) of independent biological replicates. $^{**}P < 0.01$ indicates significant differences from the control.

WRKY33SD (SD) but not WRKY33SA (SA) overexpression induces *RAP2.2* expression and enhances tolerance to DS

WRKY33 plays a key role in defense pathways, acting via MPK3/MPK6-mediated phosphorylation (Mao et al., 2011; Li et al., 2012). Since the mitogen-activated kinases MPK3/MPK6 positively regulate the hypoxia response (Chang et al., 2012), together with our finding that WRKY33 also positively participates in the submergence response and the possibility that submergence treatment induces the posttranscriptional modification of WRKY33, we investigated whether submergence would alter the phosphorylation level of WRKY33 and if so, whether this is mediated by MPK3/MPK6. First, using a gel containing phos-tag, we separated phosphorylated WRKY33 from non-phosphorylated WRKY33 isolated from *WRKY33OE* plants subjected to DS treatment and during the reoxygenation process (Figure 6A). Immunoblotting showed that phosphorylated WRKY33 started to accumulate at 2 h, which continued up to 20 h of DS treatment but gradually decreased during the reoxygenation process (Figure 6, A–B), suggesting that phosphorylated WRKY33 may participate in the submergence response. Second, to determine whether MPK3/MPK6 phosphorylate WRKY33, we generated *35S:FLAG-WRKY33SA* overexpressing transgenic plants (*SAOE*) (created by changing Ser54, Ser59, Ser65, Ser72, and Ser85 to alanine, which blocks the phosphorylation of WRKY33 (WRKY33-P) by MPK3/MPK6 (Mao et al., 2011)) and *35S:FLAG-WRKY33SD* overexpressing transgenic plants (*SDOE*) (in which Ser54,

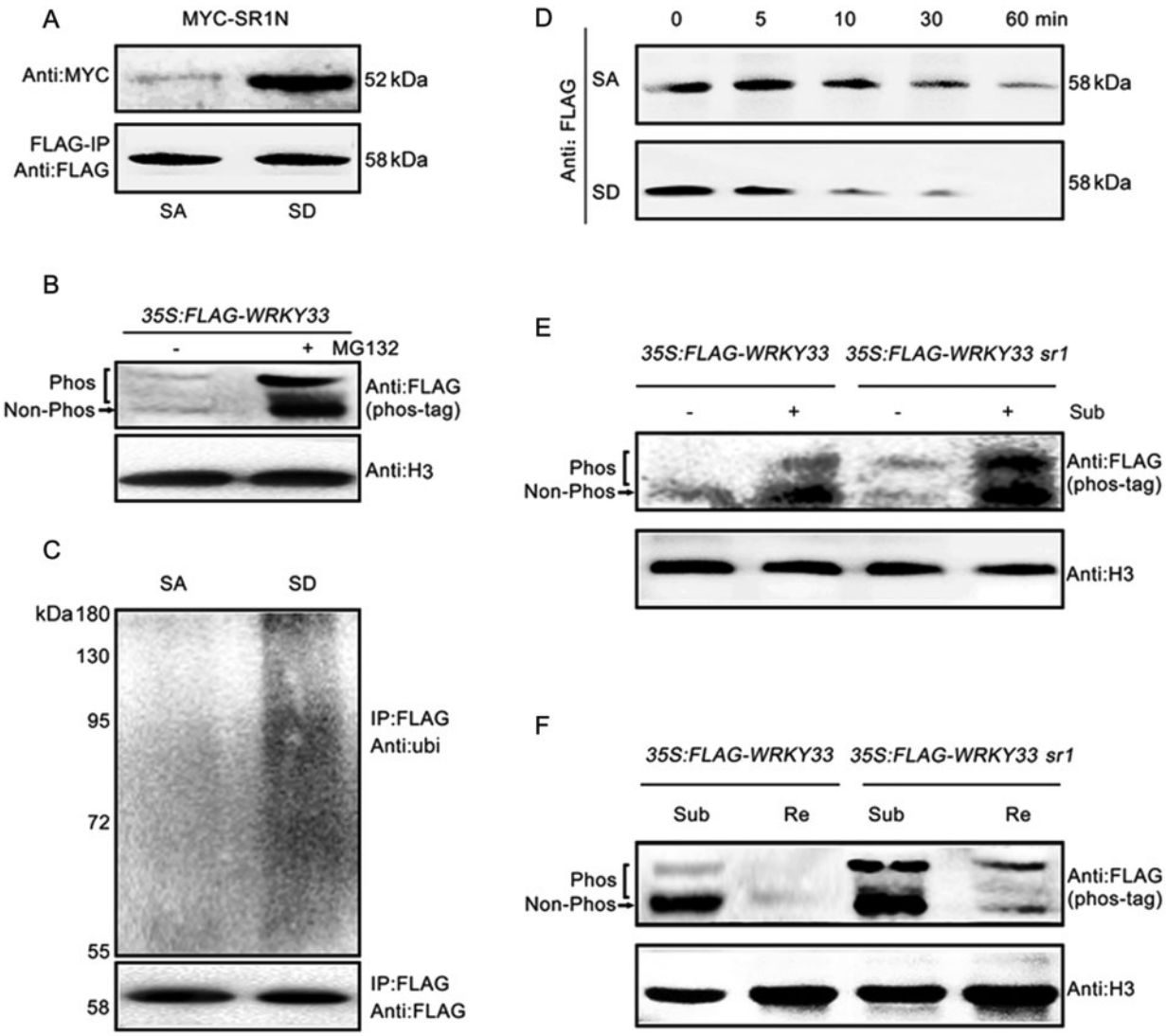

Figure 8 Phosphorylation stimulates WRKY33 turnover and is dependent on SR1. (A) FLAG-IP experiment to examine the interaction between SR1 and SA or SD. Nuclear proteins were isolated from *N. benthamiana* leaves after expressing *35S:MYC-SR1N* and *35S:FLAG-SA* or *35S:MYC-SR1N* and *35S:FLAG-SD* for 3 days. Anti:FLAG antibody conjugated agarose beads were used for the IP experiment. Anti:MYC and anti:FLAG antibodies were used for immunoblot analysis. (B) Effects of MG132 on the stability of the phosphorylated form of WRKY33. Nuclear proteins were isolated from leaves of 3-week-old *35S:FLAG-WRKY33* seedlings after treatment with or without 50 μM MG132 for 24 h and detected using a 7.5% phos-tag gel. Anti:FLAG and anti:H3 antibodies were used for immunoblot analysis. (C) Ubiquitination levels of SD and SA proteins detected in vivo. Anti:FLAG antibody-conjugated agarose beads were used for the IP experiment. Anti:ubi antibody was used to detect the levels of WRKY33 ubiquitination. Anti:FLAG antibody was used to check loading levels. (D) Nuclear proteins were extracted from 3-week-old seedlings of *35S:FLAG-SD* and *35S:FLAG-SA* in a buffer supporting proteasome activity. Extracts were incubated at room temperature for the time periods indicated. Immunoblot analysis was then performed using anti:FLAG antibody. (E) The levels of phosphorylated WRKY33 protein detected following dark submergence treatment. Nuclear proteins were extracted from 3-week-old seedlings of *35S:FLAG-WRKY33* and *35S:FLAG-WRKY33 sr1* plants after dark submergence treatment for 20 h (dark air was used as the control(-)). Phosphorylated proteins were detected using a 7.5% phos-tag gel. Anti:FLAG and anti:H3 antibodies were used for immunoblot analysis. (F) WRKY33 protein levels were examined after 2 h dark submergence treatment and reoxygenation for 14 h. Nuclear proteins were extracted from 3-week-old rosette leaves of *35S:FLAG-WRKY33* and *35S:FLAG-WRKY33 sr1* plants. Phosphorylated proteins were detected using a 7.5% phos-tag gel. Anti:FLAG and anti:H3 antibodies were used for immunoblot analysis. The molecular weight of FLAG-WRKY33, FLAG-SA or FLAG-SD is 58 kDa, MYC-SR1N is 52 kDa.

Ser59, Ser65, Ser72, and Ser85 were changed to aspartic acid, which mimics the constitutive WRKY33-P by MPK3/MPK6; Figure 6C). Phenotypic analysis showed that *SDOE* plants exhibited significantly enhanced tolerance of DS treatment, whereas *SAOE* plants did not exhibit any difference in submergence tolerance compared to wild-type Col (Figure 6D). This result was further verified by measuring survival rates (Figure 6E) and DWs (Figure 6F).

Since WRKY33 may directly up-regulate *RAP2.2* via its W box, we examined the expression of *RAP2.2* in *SDOE* and

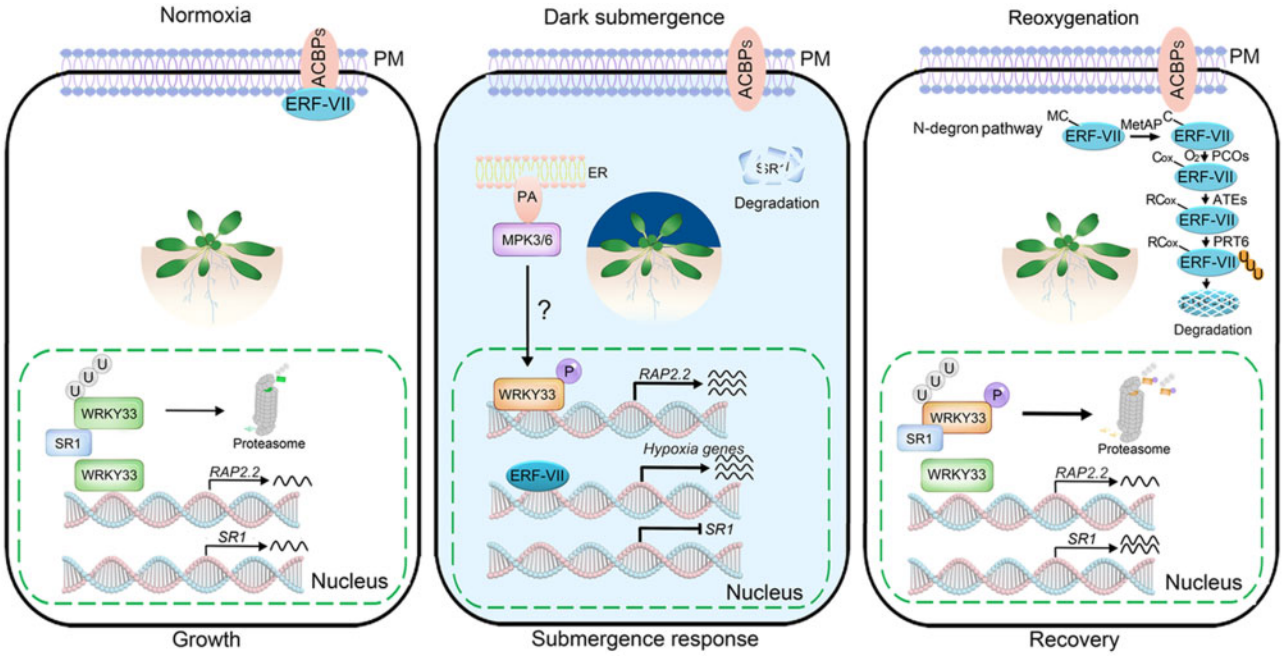

Figure 9 Working model for the role of SR1 in regulating the dark submergence response by modulating the stability of WRKY33. Under normoxia, *SR1* is constitutively expressed and SR1 is stable. WRKY33 undergoes partial degradation by SR1 to maintain dynamic equilibrium; WRKY33 can bind to the *RAP2.2* promoter to maintain its constitutive expression. RAP2.2 and other members of the ERF-VII family are normally localized to the plasma membrane where they interact with the membrane-associated ACBP1 and ACBP2. Upon exposure to hypoxia induced by dark submergence, ERF-VII proteins dissociate from the membrane and are translocated into the nucleus to activate the expression of hypoxia-response genes. WRKY33 is simultaneously phosphorylated, possibly by MPK3/MPK6 (MPK3/6), and translocated into the nucleus to strongly activate *RAP2.2* expression. In addition, *SR1* is repressed and SR1 protein is degraded by an unknown mechanism, ensuring the stabilization of WRKY33-P. After dark submergence is replaced by reoxygenation, ERF-VII proteins are degraded via the N-degron pathway while WRKY33-P is simultaneously degraded by the rapidly accumulated SR1.

SAOE plants as well as the ability of SD and SA proteins to bind to the *RAP2.2* promoter. *RAP2.2* was significantly up-regulated in *SDOE* plants, as revealed by qRT-PCR (Figure 7A), whereas overexpression of *SA* had no effect on *RAP2.2* expression compared to wild-type Col plants (Figure 7A). ChIP-qPCR analysis showed that SD could bind to the W box in the *RAP2.2* promoter at levels comparable to SA in vivo (Figure 7, B–C; Supplemental Figure S25). This result was supported by an EMSA (Figure 7, D–F) in which equal amounts of purified MBP-SD and MBP-SA proteins were loaded (Supplemental Figure S26). In addition, a dual-luciferase experiment showed that the ability of SD to activate *LUC* driven by the *RAP2.2* promoter was abolished when SR1 was added, whereas we did not detect the activation of *RAP2.2* by SA (Figure 7G–H; Supplemental Figure S27). Collectively, these results indicate that submergence induces the WRKY33-P, likely via the mitogen-activated kinases MPK3/MPK6, which might affect the transactivation activity rather than the DNA binding activity of WRKY33 and confer submergence resistance, at least in part by directly up-regulating *RAP2.2*.

Phosphorylation stimulates WRKY33 turnover and is dependent on SR1

As WRKY33 can be degraded by the 26S proteasome via SR1, we investigated whether this was also the case for the phosphorylation-blocked form SA and the phosphorylation mimic form SD. First, to examine the effect of phosphorylation on the interaction between WRKY33 and SR1, we performed an IP experiment. The constitutively phosphorylated form SD interacted with SR1 more strongly compared to SA (Figure 8A). E3 ligase facilitated the degradation of its targets, and SD had a stronger interaction with SR1, suggestion that the rate of degradation of SD might be faster than that of SA. To confirm this notion, we employed MG132, finding that the degradation of WRKY33-P was blocked by MG132 treatment (Figure 8B). Polyubiquitination of FLAG-SA protein was markedly reduced compared to FLAG-SD in the IP assay (Figure 8C). Moreover, in a cell-free degradation assay, the FLAG-SD protein showed an increased degradation rate compared to FLAG-SA (Figure 8D). Thus, we suggest that WRKY33-P may be the major form of this protein regulated by the E3 ligase SR1.

Finally, as showed that reoxygenation after DS treatment increased the protein level of SR1 (Figure 4A) and decreased the protein level of WRKY33 (Figure 4B), we performed immunoblot analysis to examine the roles of these proteins in the reoxygenation process. As shown in Figure 8, E and F, submergence treatment induced the accumulation of WRKY33-P, especially in the *sr1* mutant in which *SR1* was barely expressed (Figure 8E). WRKY33-P was clearly degraded during the reoxygenation process in Col but not in the *sr1* mutant (Figure 8F). These

findings suggest that SR1 is responsible for the degradation of WRKY33-P both in response to submergence treatment and during the reoxygenation process. Overall, our results suggest that the submergence response, which restricts plant growth, is abolished by the degradation of WRKY33-P, a process mediated (at least in part) by the E3 ligase SR1.

Discussion

Oxygen is critical for the survival of plants, which depend on molecular oxygen to produce respiratory energy. When oxygen is limited due to waterlogging or flooding, various acclimation mechanisms exist to reduce hypoxia damage. ERF-VII TFs are master regulators that activate hypoxia-response genes in *Arabidopsis* (Hinz et al., 2010; Gibbs et al., 2011; Licausi et al., 2011; GiuntoLi et al., 2017; Gibbs and Holdsworth, 2020). In this study, we found that the ERF-VII family member *RAP2.2* is strongly activated by a phosphorylated form of WRKY33 that binds to the W box cis-element present in its promoter. We demonstrated that the ubiquitin E3 ligase SR1 negatively regulates the submergence response by degrading phosphorylated WRKY33 during reoxygenation. These findings indicate that the on-and-off module SR1-WRKY33-*RAP2.2* replenishes and is connected with the well-known N-degron pathway based on ERFVII family members that function in the plant submergence response (Figure 9).

WRKY33 is a positive regulator of plant defense responses (Zheng et al., 2006; Lai et al., 2011; Liu et al., 2015) and is also involved in responses to various abiotic stresses (Jiang and Deyholos, 2009; Datta et al., 2015; Zhou et al., 2015; Liao et al., 2016; Tang et al., 2020). *WRKY33* is also induced after hypoxia treatment or submergence in *Arabidopsis* (Klok et al., 2002; Tang et al., 2020; Supplemental Figure S16). In the current study, we found that submergence induced the WRKY33-P, which then conferred enhanced submergence tolerance by strongly activating the ERF-VII family gene *RAP2.2* (Figure 7). The WRKY33-P may be carried out by the mitogen-activated kinases MPK3/MPK6 in *Arabidopsis*, as has been observed in other abiotic stress responses (Mao et al., 2011; Chang et al., 2012), although it remains unknown whether other phosphorylation sites are activated by other kinases. Nonetheless, our study also supports the previous finding that WRKY33 is a core positive regulator of responses to diverse stresses (Zheng et al., 2006; Lai et al., 2011; Mao et al., 2011; Chang et al., 2012; Liu et al., 2015; Tang et al., 2020). However, the genes targeted and the modes of regulation with or without posttranslational modification vary greatly, depending on the nature of the stress.

E3 ligases are important posttranslational ubiquitination enzymes that function in various stress responses, such as the abscisic acid signaling pathway (Ding et al., 2015a, 2015b; Lee and Seo, 2016) and the cold stress response pathway (Ding et al., 2015a, 2015b; Li et al., 2017; Wang et al., 2019). For example, the N-degron pathway E3 ligase PROTEOLYSIS6 and two E3 ligases, the RING domain-containing proteins SEVEN IN ABSENTIA of ARABIDOPSIS1 (SINAT1) and SINAT2, participate in the hypoxia response by regulating the stability of RAP2.12 (Gibbs et al., 2011; Licausi et al., 2011; Papdi et al., 2015; Gibbs and Holdsworth, 2020). In this study, we provide evidence that an additional E3 ligase, SR1, directly interacts with and degrades WRKY33-P to negatively regulate the submergence response (Figure 8). The N terminal region of this SR1, which contains a zinc-finger domain, might interact with the C terminal region of WRKY33 (Figure 3) during the submergence-reoxygenation response, although the precise identification of functional sites and other potential targeted regions requires further study. The expression of SR1 was negatively correlated with that of WRKY33-P during submergence-reoxygenation, but with a delay (Figure 4, A and B). This delayed expression suggests that additional partners or modifications may be needed for SR1 to remove WRKY33-P. The degradation of WRKY3-P (Figure 4; Supplemental Figure S16) suggests the existence of another pathway for sensing oxygen during reoxygenation. We showed that WRKY33-P is degraded by the rapidly accumulated E3 ligase SR1, acting as a non-canonical oxygen sensing mechanism. This differs from the removal of ERF-VIIs during aerobic restoration through the oxygen sensing and N-degron pathways (Gibbs et al., 2011; Licausi et al., 2011; Gibbs and Holdsworth, 2020). However, it remains unknown how SR1 senses oxygen to initialize ubiquitination of WRKY33-P and how it is itself removed when submergence ends.

Overall, we identified a submergence resistant mutant, *sr1*, and clarified the role played by SR1 as a negative regulator of the submergence response via degradation of WRKY33-P. Our findings indicate that the PA-MPK3/MPK6 (Yu et al., 2010; Chang et al., 2012; Xie et al., 2020) and N-degron pathways (Gibbs et al., 2011; Licausi et al., 2011; Gibbs and Holdsworth, 2020) are connected via WRKY33-P to trigger a high expression level of *RAP2.2* during hypoxia acclimation (Figure 9). Under normoxia, *SR1*, *WRKY33*, and *RAP2.2* are constitutively expressed to maintain dynamic equilibrium. RAP2.2 and other ERF-VII proteins are localized to the plasma membrane where they interact with the membrane-associated proteins ACYL-COA BINDING PROTEIN1 (ACBP1) and ACBP2 (Licausi et al., 2011; Bailey-Serres et al., 2012a, 2012b; Xie et al., 2020). Upon exposure to hypoxia, WRKY33 is phosphorylated by PA-MPK3/MPK6, and *RAP2.2* expression is enhanced to promote acclimation. However, both WRKY33-P and RAP2.2 are simultaneously degraded by SR1 and the N-degron pathway during reoxygenation. This SR1-WRKY33-*RAP2.2* regulatory module connects the known oxygen sensing and N-degron pathways but represents another signal transduction pathway that operates during submergence acclimation in *Arabidopsis*. Such rapid and precise activation and removal of submergence-response proteins can effectively balance plant growth and stress acclimation. These findings suggest that the submergence response and oxygen perception in plants may be even more interesting than previously believed; further studies of this topic are needed. In

addition, our identification of SR1 and WRKY33 as two key submergence-resistant targets provides a basis for genetic manipulation for biotechnology-based breeding of crops with improved flooding tolerance.

Materials and methods

Plant materials and growth conditions

To generate *A. thaliana* *35S:FLAG-WRKY33*, *35S:FLAG-SA*, *35S:FLAG-SD*, *35S:SR1*, *35S:FLAG-SR1*, and *35S:RAP2.2* overexpressing transgenic plants, the *WRKY33*, *SA*, *SD*, *SR1*, and *RAP2.2* coding sequences (CDS) were amplified and cloned into the pCAMBIA1300 or pCAMBIA1300-FLAG vector through the *XbaI* and *KpnI* sites using a ClonExpress II One Step Cloning Kit (C112-01; Vazyme, Nanjing, China). To generate *pSR1:SR1/sr1* and *pSR1:GUS* transgenic plants, the 1 kb promoter sequence of *SR1* (Maher et al., 2018) together with the full-length CDS of *SR1* was amplified and cloned into the pBIB-BASTA-35S-GWR-GFP and pCXGUS-P vectors through the *KpnI* and *BamHI* sites using the same cloning kit (C112-01, Vazyme). All primers used in this study are listed in Supplemental Table S1, and all transgenic plants used are listed in Supplemental Table S2. Agrobacterium carrying *35S:FLAG-WRKY33*, *35S:FLAG-SA*, *35S:FLAG-SD*, *35S:SR1*, *35S:FLAG-SR1*, *35S:RAP2.2*, *pSR1:SR1*, and *pSR1:GUS* constructs was transformed into *Arabidopsis* ecotype Col-0 or the *sr1* background via the floral dip method (Zhang et al., 2006) and identified by hygromycin screening followed by qRT-PCR analysis of the expression levels of the relevant genes. The T-DNA insertional mutants of genes, including *AT1G14770* (SALK_038318), *AT4G09110* (CS55893), *AT3G45480* (SALK_093138, CS927049), *AT5G36001* (SALK_012983), *AT5G22920* (CS424220), *wrky33* (SALK_006603), and *sr1* (SALK_076386), were obtained from the Arabidopsis Biological Resource Center (ABRC). *sr1 wrky33* and *RAP2.2OE wrky33* plants were generated by genetic crossing, followed by genomic identification. F3 populations of the crossed lines were used in all experiments.

Seeds were surface-sterilized with 10% NaClO for 10 min and washed 6 times with sterilized distilled water. Surface-sterilized seeds were sown on half-strength Murashige and Skoog medium (Sigma-Aldrich, St. Louis, MO, USA) plates with 2% sucrose solidified with 0.75% agar (pH 5.85) and grown in a growth chamber under a 16 h light/8 h dark (22°C) cycle with fluorescent white light at 13,700 lux (Philips F17T8/TL841 17W). Seedlings were transplanted into soil at the two-leaf stage for subsequent growth under the same conditions.

Submergence stress and hypoxia treatment

For submergence treatment, 3-week-old plants were dark-submerged in deionized water (with leaves 10 cm below the water surface) in the same dark plastic box for the times indicated. All submergence treatments began at 9:00 a.m., which was the start of the 16 h light/8 h dark (22°C) cycle. After dark-submergence treatment, water was removed and plants were returned to normal growth conditions (16/8 h light/dark cycles; 22°C) for the times indicated. Flooding tolerance was assayed using at least two independent lines of each transgenic genotype, and similar results were obtained, so representative results obtained with only one line are presented here. Then 12–30 plants per genotype were used each time, and three repetitions were done.

For hypoxia treatment, 10–20 1-week-old seedlings were placed in an enclosed anaerobic workstation in the dark, and hypoxic conditions (1% oxygen) were achieved by constantly bubbling 99.999% nitrogen into the chamber for 12 h. GUS staining was carried out after hypoxia treatment. For comparison, 10–20 1-week-old seedlings without hypoxia treatment were also subjected to GUS staining.

Dry weight, ion leakage assays, and MDA measurements

For DW measurements, above-ground tissues of 3-week-old plants were weighed after heating at 65°C for 2 days. The DW of 10–20 plants after submergence treatment followed by 5 days of reoxygenation was recorded.

For ion leakage measurements, 3-week-old rosette leaves of 10–20 plants subjected to different treatments were collected into 15 mL tubes, each containing 10 mL deionized water, and shaken for 1 h at room temperature. Initial conductivity (S1) of the samples was measured with a conductivity meter. The samples were boiled for 10 min, cooled to room temperature, and incubated with shaking for another 10 min before measuring the final conductivity (S2). Ion leakage was calculated as S1/S2.

For MDA measurements, 3-week-old rosette leaves of 10–20 plants exposed to different treatments were weighed and pulverized in 5% trichloroacetic acid buffer, and the supernatant was mixed with 6.7% thiobarbituric acid and 5% trichloroacetic acid buffer. After 30 min incubation at 100°C, the samples were cooled to room temperature, and absorbance was measured at 532, 450, and 600 nm with a spectrophotometer plate reader.

Subcellular localization

The *35S:SR1-GFP* and *35S:GFP* plasmids were transformed into *Arabidopsis* protoplasts, which were prepared from 2-week-old wild-type (Col-0) *Arabidopsis* rosette leaves. *Arabidopsis* protoplasts were isolated and transfected using 10 μg of each plasmid DNA at a concentration of 1 μg/μL as previously described (Liu et al., 2014). GFP fluorescence was visualized under a laser-scanning confocal microscope (Leica TCS SP5) 24 h after transfection. At least 10 cells were observed for each experiment, and they all showed a similar expression pattern.

Phylogenetic analysis

Protein homology searches were performed with the Phytozome program (http://www.phytozome.net/). Selected AA sequences from *Arabidopsis*, rice (*Oryza sativa*), maize (*Zea mays*), soybean (*Glycine max*), and poplar (*Populus*) were aligned using ClustalW. The alignment is available as Supplemental File S1. Phylogenetic trees were generated using the neighbor-joining method with the MEGA version

5.10 software package. Bootstrap values were supported by 10,000 replicates. Branch length indicates divergence distance. Numbers on the branches indicate percentage bootstrap support.

Y2H screening and assays

A cDNA library was constructed from the leaves of 2-week-old Col treated with 24 h of DS following the Matchmaker™ Gold Y2H System procedure (Clontech, Mountain View, CA, USA). Y2H screening was performed 3 times, and WRKY33 was identified twice as a putative interaction partner of SR1. Five cDNA clones encoding WRKY33 (among the 3 times) were identified in the Y2H screening. Other proteins (such as those encoded by AT5G58410, AT3G11280, AT5G39360, AT1G01720, and AT5G13810) were also identified as candidate partners during the screening. Y2H analysis was performed to verify the interaction between SR1 and the candidate, WRKY33. Full- or partial-length cDNAs from *WRKY33* or *SR1* genes were fused into, respectively, the GAL4 AD vector (pGADT7) or the GAL4 BD vector (pGBKT7), to obtain the constructs *BD-WRKY33*, *BD-SA*, *BD-SD*, *BD-WRKY33N*, *BD-WRKY33C*, *AD-SR1*, *AD-SR1N*, and *AD-SR1C*. Two constructs (using 4 μL of each plasmid DNA at a concentration of 500 ng/μL) were co-transformed into yeast strain AH109, and transformants were selected based on growth on selective dropout medium SD-LTHA (lacking leucine, tryptophan, histidine, and alanine) to determine their growth status.

qRT-PCR analysis

Total RNA was extracted from rosette leaves of 3-week-old plants using TRIzol reagent (BioFit Bowling Green, OH, USA; Cat# RN33). About 2 μg of RNA was reverse transcribed using a PrimeScript RT reagent kit (Takara, Kyoto, Japan; Cat# RR047A). The *Arabidopsis ACTIN* gene was used as the internal reference. A QuantiNova SYBR Green PCR Kit was used for qRT-PCR with specific primers (Supplemental Table S1). A Bio-Rad CFX96 Real-Time System was used for analysis. The relative expression levels were calculated as described previously (Miura et al., 2007).

GUS and DAB staining

Plant material produced under the same growth conditions but different treatments (with or without DS treatment for 20 h) was stained in 50 mM GUS staining solution at 37°C for 3 h and immersed in absolute ethanol overnight to remove the chlorophyll and staining solution prior to photography. GUS staining solution (Solarbio, Beijing, China; G3061) was used in this assay.

For DAB staining, 3-week-old rosette leaves subjected to 2 or 20 h DS, or without DS treatment, were collected and stained in 1 mg/mL DAB staining solution in the dark for 3 h and immersed in absolute ethanol overnight prior to photography. DAB (BOSTER, Pleasanton, CA, USA; AR1000) was used in this assay.

Nuclear protein extraction and immunoblotting

Rosette leaves of 3-week-old *Arabidopsis* plants grown in soil were ground and incubated in nuclear extraction buffer (20 mM HEPES PH 7.5, 40 mM KCl, 10 mM $MgCl_2$, 1% TritonX-100, 1 mM EDTA, 10% glycerin, 1 mM PMSF, 1 × Cocktail, 10 μM MG132) (Zhang et al., 2012), filtered through three layers of Miracloth (Calbiochem, San Diego, CA, USA), and centrifuged at 4,000 *g* for 5 min at 4°C. The supernatant was discarded, and the precipitate (containing nuclear protein) was retained for further experimentation.

Immunoblotting was performed according to the *Molecular Cloning* manual. Proteins were boiled in SDS sample buffer at 95°C for 5–10 min. Samples were cooled on ice for 1–2 min and centrifuged for 1 min at 12,000 g. Twelve percentage SDS-PAGE gels were used in most cases, while 15% SDS-PAGE gels were used to detect histone H3. Anti:H3 (Abbkine, CA, USA; cat#: ABP53164), anti:FLAG (Sigma-Aldrich; F9291), anti:ubi ((P4D1): sc-8017; Santa Cruz Biotech, Dallas, TX, USA), anti:MBP (New England Biolabs, Ipswich, MA, USA), anti:GST (Sangon Biotech, Shanghai, China), anti:His (Sangon Biotech), anti:MYC (9E10; Abcam, Cambridge, UK) and anti:HA (ab9110; Abcam) antibodies were used.

Protein degradation assays

For the cell-free degradation assays (Spoel et al., 2009), nuclear protein was extracted from 3-week-old seedlings in buffer containing 25 mM Tris–HCl pH 7.5, 10 mM $MgCl_2$, 10 mM NaCl, and 10 mM ATP. After centrifugation (14,000 *g*, 10 min, 4°C), the supernatants were incubated at 25°C and the reactions terminated by adding SDS sample buffer and boiling at 95°C for 10 min.

Pull-down and BiFC assays

For pull-down assays, the *SR1* N terminal and *WRKY33* full-length coding regions were cloned into the pGEX4T-1 (containing a GST tag) and pMAL-p4x (containing an MBP tag) vectors, respectively. The recombinant GST-SR1N and MBP-WRKY33 proteins were purified using Glutathione-Sepharose beads (GE) and amylose resin (New England Biolabs), respectively. MBP-WRKY33 or the MBP protein alone was immobilized with amylose resin (New England Biolabs) and incubated with GST-SR1N in incubation buffer (25 mM Tris–Cl, 150 mM NaCl, 1 mM EDTA; pH 7.4) with gentle agitation (4°C; 3 h). After washing 5 times, 1 × SDS loading buffer was added to the bead-retained proteins, and the samples were boiled for 5 min, separated by 12% SDS-PAGE, and visualized by immunoblot analysis with anti:MBP (New England Biolabs) and anti:GST (Sangon Biotech) antibodies.

BiFC assays were performed as previously described (Lee et al., 2008). Full-length *WRKY33* or *SR1* cDNA was cloned and fused with the N-terminus of YFP (WRKY33-nVenus) or the C-terminus of YFP (SR1-cCFP). *Arabidopsis* protoplasts were isolated and transfected (using 10 μg of each plasmid

DNA at a concentration of 1 μg/μL) as previously described (Liu et al., 2014). YFP fluorescence was visualized under a laser-scanning confocal microscope (Leica TCS SP5) 24 h after transfection.

IP assay

For Co-IP analysis, Agrobacterium carrying the *35S:MYC-SR1N* and *35S:FLAG-WRKY33* constructs was introduced into 3-week-old *N. benthamiana* leaves. After incubating the leaves for 2 days in darkness and 1 day under normal growth conditions (a 16 h light/8 h dark [22°C] cycle with fluorescent white light at 13,700 lux [Philips F17T8/TL841 17 W]), nuclear protein was isolated (Zhang et al., 2012) in nuclear extraction buffer (20 mM HEPES pH 7.5, 40 mM KCl, 10 mM $MgCl_2$, 1% TritonX-100, 1 mM EDTA, 10% glycerin, 1 mM PMSF, 1 × Cocktail, 10 μM MG132).

For IP analysis alone, nuclear protein was isolated from plant material (Zhang et al., 2012) in nuclear extraction buffer. After isolation, the protein was centrifuged at 12,000 rpm for 10 min and resuspended in 70 μL nuclear lysis buffer (50 mM Tris–HCl pH 8.0, 10 mM EDTA, 0.1% SDS) for 10 min at 4°C prior to the addition of 600 μL dilution buffer (16.7 mM Tris–HCl pH 8.0, 16.7 mM NaCl, 1.2 mM EDTA, 0.01% SDS). An ultrasonicator was used to release nuclear protein with a cycle of 8 s sonication, 30 s rest, repeated 8 times, at 4°C. Released nuclear proteins were mixed with 20 μL anti:FLAG beads (ab1240; Abcam) and incubated at 4°C for 2 h. After washing, the IP products were boiled at 95°C for 10 min. Samples were separated by 12% SDS-PAGE and subjected to immunoblot analysis.

In vitro ubiquitination assays

Equal amounts of GST-SR1N, His-UBI, UBCH5C (E2), and E1 (R&D Systems, E-300-050) were added to each reaction. GST-SR1N and His-UBI were expressed in *Escherichia coli* Rosetta2 (DE3) strain *BL21* induced with 0.5 mM isopropyl β-D-1-thiogalactopyranoside (IPTG) by incubation at 16°C for 15 h. The reactions were performed in buffer containing 50 mM Tris–HCl (pH 7.5), 10 mM phosphocreatine (Solarbio), 5 mM $MgCl_2$, 5 mM ATP, 1 mM DTT, and 1 unit of creatine kinase (Solarbio), incubated at 30°C for 2 h. The reactions were stopped by adding 5 × SDS loading buffer and incubating at 95°C for 5 min and analyzed by 12% SDS-PAGE. Anti:His (Sangon Biotech) and anti:GST (Sangon Biotech) antibodies were used in the immunoblot assays.

In vivo phosphorylation assay

Nuclear proteins were extracted from the leaves of 3-week-old *35S:FLAG-WRKY33* seedlings. And 7.5% phos-tag gel (WAKO, Richmond, VA, USA; 198-17981) was used to separate the phosphorylated and non-phosphorylated forms of WRKY33. Samples from different treatments were suspended in 1 × SDS sampling buffer with 1 × phosphatase inhibitor cocktail (Bimake, Houston, TX, USA; b15001) and 1 × protease inhibitor cocktail, EDTA-free (Bimake; b14001). Electrophoresis was performed in running buffer (25 mM Tris, pH 8.8, 20 mM Glycine, 0.1% SDS) at 120 V for 1 h. The gel was soaked in transfer buffer (25 mM Tris, 20 mM Glycine) with 10 mM EDTA for 20 min 3 times with gentle agitation, washed in transfer buffer without EDTA for another 10 min, and the proteins from the gel transferred to a membrane at 120 mA for 2 h. Anti:FLAG (1:1000, Sigma-Aldrich; F1084) antibody was used in the immunoblot assay.

EMSA

Different forms of WRKY33 were introduced into the PET28a vector to obtain His-WRKY33, His-WRKY33SA, and His-WRKY33SD proteins. All proteins were expressed in *E. coli* Rosetta2 (DE3) strain *BL21* induced with 0.5 mM IPTG by incubation at 16°C for 15 h. Biotin-labeled fragments (5′-ATTTCTAAGGACAGTCAAATATGACAACAT-3′ with one W box element and 5′-ATTTCTAAGGACAAAAAAATA TGACAACAT-3′ with mutations in the W box element) were used as the biotin probes. Un-labeled fragments were used as cold probes. The biotin-labeled probes were synthesized at Sangon Biotech. EMSAs were performed using a LightShift Chemiluminescent EMSA kit (Thermo Fisher, Waltham, MA, USA).

Dual-luciferase assays

A dual-luc activity assay was performed using young *N. benthamiana* leaves (Hellens et al., 2005). Then 1 kb of the *RAP2.2* promoter was inserted into the pGreen-0800-LUC vector to use as a reporter. The Renilla luciferase (*REN*) gene was used as the internal control, and *35S:FLAG-WRKY33*, *35S:FLAG-WRKY33SA*, *35S:FLAG-WRKY33SD*, and *35S:FLAG-SR1* were the effectors. Equal amounts of *A. tumefaciens* strain GV3101 carrying different constructs were co-injected into 3-week-old *N. benthamiana* leaves. Luciferase and Renilla luciferase activities were measured with a Dual-luciferase Reporter Assay System (Promega, Madison, WI, USA) after 2 days of incubation in the dark and 1 day of cultivation under normal growth conditions.

ChIP-qPCR analysis

DNA-protein complexes were extracted from rosette leaves of 3-week-old *35S:FLAG-WRKY33*, *35S:FLAG-WRKY33SA*, and *35S:FLAG-WRKY33SD* transgenic plants, and pulled down using anti:FLAG antibody and protein A Agarose beads following the ChIP protocol (Bowler et al., 2004). Amounts of the DNA-protein complexes that were pulled down were calculated relative to 10% of the total DNA and protein complexes before the pull-down experiment. The immunoprecipitated DNA fragments were detected by qRT-PCR as previously described (Liu et al., 2014). The specific primers used for ChIP-qPCR are listed in Supplemental Table S1. A fragment in the CDS of *RAP2.2* was used as a negative control.

Statistical analysis

The data in this study are expressed as ±SD of three independent biological replicates unless otherwise indicated. The two-tailed Student's *t*-test method was used to calculate the significance of differences between groups. *P*-values < 0.05 or < 0.01 were considered significant.

Accession numbers

Sequence data from this article can be found in the *Arabidopsis* Genome Initiative or GenBank/EMBL databases under the following accession numbers: *SR1* (*AT2G47090*), *WRKY33* (*AT2G38470*), *ADH1* (*AT1G77120*), *PDC1* (*AT4G33070*), *SUS4* (*AT3G43190*), *PCO2* (*AT5G39890*), *LBD41* (*AT3G02550*), *HB1* (*AT2G16060*), *ACS2* (*AT1G01480*), *SRH1* (*AT3G62240*), *RAP2.2* (*AT3G14230*), *RAP2.12* (*AT1G53910*), *HRE1* (*AT1G72360*), and *HRE2* (*AT1G72360*).

Supplemental Data

The following supplemental materials are available in the online version of this article.

Supplemental Figure S1. Relative expression levels of hypoxia-responsive genes encoding potential E3 ligases.

Supplemental Figure S2. Identification of the *sr1* mutant.

Supplemental Figure S3. Identification of *SR1*-overexpressing transgenic plants and *pSR1: SR1/sr1* transgenic lines.

Supplemental Figure S4. Electrolyte leakage and water loss of Col, *sr1*, *pSR1:SR1/sr1*, and *SR1OE* plants.

Supplemental Figure S5. Relative expression levels of hypoxia-responsive marker genes.

Supplemental Figure S6. Phylogenetic analysis of *SR1* and expression analysis of the homolog of *SR1* (*SRH1*) in response to DS and re-oxygenation treatment.

Supplemental Figure S7. *SR1* expression analysis by GUS staining.

Supplemental Figure S8. Expression patterns of *SR1* in different tissues analyzed by qRT-PCR.

Supplemental Figure S9. SRH1 does not interact with WRKY33 in a Y2H assay.

Supplemental Figure S10. Identification of *35S:FLAG-SR1*-overexpressing transgenic plants.

Supplemental Figure S11. Identification of *35S:FLAG-WRKY33*-overexpressing transgenic plants.

Supplemental Figure S12. *FLAG-SR1* and *FLAG-WRKY33* mRNA levels are not affected by DS treatment.

Supplemental Figure S13. MG132 treatment prevents the degradation of SR1 during DS.

Supplemental Figure S14. *FLAG-WRKY33* mRNA levels in *35S:FLAG-WRKY33* and *35S:FLAG-WRKY33 sr1* plants detected by qRT-PCR.

Supplemental Figure S15. Relative expression levels of *FLAG-WRKY33* and *MYC-SR1N* in transient expression assays detected by qRT-PCR.

Supplemental Figure S16. WRKY33 positively regulates the DS response in *Arabidopsis*.

Supplemental Figure S17. Relative expression levels of hypoxia-responsive marker genes in Col, *wrky33*, and *WRKY33OE* plants.

Supplemental Figure S18. Relative expression levels of hypoxia-responsive marker genes in Col, *sr1*, *wrky33*, and *sr1 wrky33* plants.

Supplemental Figure S19. Relative expression levels of *RAP2.12*, *HRE1*, *HRE2*, *RAP2.2* in Col, *wrky33*, and *WRKY33OE* plants.

Supplemental Figure S20. Relative expression levels of *RAP2.2*, *RAP2.12*, *HRE1*, *HRE2* in Col, *sr1*, and *SR1OE* plants.

Supplemental Figure S21. Relative expression levels of *RAP2.2* in Col, *sr1*, *wrky33*, and *sr1 wrky33* plants.

Supplemental Figure S22. Expression patterns of *WRKY33* and *RAP2.2* in response to DS, DA, or light air (LA) treatment.

Supplemental Figure S23. *RAP2.2* functions downstream of WRKY33 to regulate the DS response.

Supplemental Figure S24. *RAP2.2* functions downstream of *WRKY33* in the DS response in *Arabidopsis*.

Supplemental Figure S25. SD/SA protein levels in *SDOE-2* and *SAOE-2* plants used for the ChIP experiment examined by immunoblotting.

Supplemental Figure S26. Quantification of the purified MBP-SD and MBP-SA proteins used in the EMSAs by immunoblotting.

Supplemental Figure S27. SD/SA protein levels in the transient expression assays shown in Figure 7H examined by immunoblotting.

Supplemental Table S1. List of primer sequences used in this study.

Supplemental Table S2. Transgenic plants used in this study

Supplemental File S1. Text file of the alignment used in the phylogenetic analysis shown in Supplemental Figure S6A.

Acknowledgments

We thank the ABRC (www.arabidopsis.org) for providing *sr1* and *wrky33* mutant seeds.

Funding

This research was supported by the Strategic Priority Research Program of Chinese Academy of Sciences (Grant No. XDB31010300), the National Natural Science Foundation of China (Grant No. 31870244, 32030006, and 31670317), and the Fundamental Research Funds for the Central Universities (2020SCUNL207, SCU2019D013).

Conflict of interest statement. The authors declare no competing interests.

References

Bailey-Serres J, Fukao T, Gibbs DJ, Holdsworth MJ, Lee SC, Licausi F, Perata P, Voesenek LACJ, van Dongen JT (2012) Making sense of low oxygen sensing. Trends Pl Sci **17**: 129–138

Bailey-Serres J, Lee SC, Brinton E (2012) Waterproofing crops: effective flooding survival strategies. Plant Physiol **160**: 1698–1709

Bowler C, Benvenuto G, Laflamme P, Molino D, Probst AV, Tariq M, Paszkowski J (2004) Chromatin techniques for plant cells. Plant J. **39**: 776–789

Chang R, Jang CJH, Branco-Price C, Nghiem P, Bailey-Serres J (2012) Transient MPK6 activation in response to oxygen

deprivation and reoxygenation is mediated by mitochondria and aids seedling survival in *Arabidopsis*. Plant Mol Biol **78**: 109–122

Datta R, Kumar D, Sultana A, Hazra S, Bhattacharyya D, Chattopadhyay S (2015) Glutathione regulates 1-aminocyclopropane-1-carboxylate synthase transcription via WRKY33 and 1-aminocyclopropane-1-carboxylate oxidase by modulating messenger RNA stability to induce ethylene synthesis during stress. Plant Physiol **169**: 2963–2981

Ding SC, Zhang B, Qin F (2015) *Arabidopsis* RZFP34/CHYR1, a ubiquitin E3 ligase, regulates stomatal movement and drought tolerance via SnRK2.6-mediated phosphorylation. Plant Cell **27**: 3228–3244

Ding YL, Jia YX, Shi YT, Zhang XY, Song CP, Gong ZZ, Yang SH (2018) OST1-mediated BTF3L phosphorylation positively regulates CBFs during plant cold responses. EMBO J **37**: e98228

Ding YL, Li H, Zhang XY, Xie Q, Gong ZZ, Yang SH (2015) OST1 kinase modulates freezing tolerance by enhancing ICE1 stability in *Arabidopsis*. Dev Cell **32**: 278–289

Gasch P, Fundinger M, Muller JT, Lee T, Bailey-Serres J, Mustroph A (2016) Redundant ERF-VII transcription factors bind to an evolutionarily conserved cis-Motif to regulate hypoxia-responsive gene expression in *Arabidopsis*. Plant Cell **28**: 160–180

Gibbs DJ, Holdsworth MJ (2020) Every breath you take: new insights into plant and animal oxygen sensing. Cell **180**: 22–24

Gibbs DJ, Lee SC, Isa NM, Gramuglia S, Fukao T, Bassel GW, Correia CS, Corbineau F, Theodoulou FL, Bailey-Serres J, et al. (2011) Homeostatic response to hypoxia is regulated by the N-end rule pathway in plants. Nature **479**: 415–418

Giuntoli B, Licausi F, van Veen H, Perata P (2017) Functional balancing of the hypoxia regulators RAP2.12 and HRA1 takes place *in vivo* in *Arabidopsis thaliana* plants. Front Plant Sci **8**: 591

Gui J, Luo L, Zhong Y, Sun J, Umezawa T, Li L (2019) Phosphorylation of LTF1, an MYB transcription factor in populus, acts as a sensory switch regulating lignin biosynthesis in wood cells. Mol Plant **12**: 1325–1337

Hattori Y, Nagai K, Furukawa S, Song XJ, Kawano R, Sakakibara H, Wu JZ, Matsumoto T, Yoshimura A, Kitano H, et al. (2009) The ethylene response factors SNORKEL1 and SNORKEL2 allow rice to adapt to deep water. Nature **460**: 1026–1030

Hellens RP, Allan AC, Friel EN, Bolitho K, Grafton K, Templeton MD, Karunairetnam S, Gleave AP, Laing WA (2005) Transient expression vectors for functional genomics, quantification of promoter activity and RNA silencing in plants. Plant Methods **1**: 13

Hinz M, Wilson IW, Yang J, Buerstenbinder K, Llewellyn D, Dennis ES, Sauter M, Dolferus R (2010) *Arabidopsis* RAP2.2: an ethylene response transcription factor that is important for hypoxia survival. Plant Physiol **153**: 757–772

Igamberdiev AU, Hill RD (2004) Nitrate, NO and haemoglobin in plant adaptation to hypoxia: an alternative to classic fermentation pathways. J Exp Bot **55**: 2473–2482

Jiang YQ, Deyholos MK (2009) Functional characterization of *Arabidopsis* NaCl-inducible WRKY25 and WRKY33 transcription factors in abiotic stresses. Plant Mol Biol **69**: 91–105

Klok EJ, Wilson IW, Wilson D, Chapman SC, Ewing RM, Somerville SC, Peacock WJ, Dolferus R, Dennis ES (2002) Expression profile analysis of the low-oxygen response in *Arabidopsis* root cultures. Plant Cell **14**: 2481–2494

Kosarev P, Mayer KFX, Hardtke CS (2002) Evaluation and classification of RING-finger domains encoded by the *Arabidopsis* genome. Genome Biol **3**: RESEARCH0016

Kraft E, Stone SL, Ma LG, Su N, Gao Y, Lau OS, Deng XW, Callis J (2005) Genome analysis and functional characterization of the E2 and RING-type E3 ligase ubiquitination enzymes of *Arabidopsis*. Plant Physiol **139**: 1597–1611

Lai ZB, Li Y, Wang F, Cheng Y, Fan BF, Yu JQ, Chen ZX (2011) *Arabidopsis* sigma factor binding proteins are activators of the WRKY33 transcription factor in plant defense. Plant Cell **23**: 3824–3841

Lee HG, Seo PJ (2016) The *Arabidopsis* MIEL1 E3 ligase negatively regulates ABA signalling by promoting protein turnover of MYB96. Nat Commun **7**: 12525

Lee LY, Fang MJ, Kuang LY, Gelvin SB (2008) Vectors for multi-color bimolecular fluorescence complementation to investigate protein-protein interactions in living plant cells. Plant Methods **4**: 1746–4811

Li GJ, Meng XZ, Wang RG, Mao GH, Han L, Liu YD, Zhang SQ (2012) Dual-level regulation of ACC synthase activity by MPK3/MPK6 cascade and its downstream WRKY transcription factor during ethylene induction in *Arabidopsis*. PLoS Genet **8**: e1002767

Li H, Ding YL, Shi YT, Zhang XY, Zhang SQ, Gong ZZ, Yang SH (2017) MPK3-and MPK6-mediated ICE1 phosphorylation negatively regulates ICE1 stability and freezing tolerance in *Arabidopsis*. Dev Cell **43**: 630–642

Liao CJ, Lai ZB, Lee S, Yun DJ, Mengiste T (2016) *Arabidopsis* HOOKLESS1 regulates responses to pathogens and abscisic acid through interaction with MED18 and acetylation of WRKY33 and ABI5 chromatin. Plant Cell **28**: 1662–1681

Licausi F, Kosmacz M, Weits DA, Giuntoli B, Giorgi FM, Voesenek LACJ, Perata P, van Dongen JT (2011) Oxygen sensing in plants is mediated by an N-end rule pathway for protein destabilization. Nature **479**: 419–422

Liu HH, Guo SY, Xu YY, Li CH, Zhang ZY, Zhang DJ, Xu SJ, Zhang C, Chong K (2014) OsmiR396d-regulated OsGRFs function in floral organogenesis in rice through binding to their targets OsJMJ706 and OsCR4. Plant Physiol **165**: 160–174

Liu SA, Kracher B, Ziegler J, Birkenbihl RP, Somssich IE (2015) Negative regulation of ABA signaling by WRKY33 is critical for *Arabidopsis* immunity towards Botrytis cinerea 2100. Elife **4**: e07295

Maher KA, Bajic M, Kajala K, Reynoso M, Pauluzzi G, West DA, Zumstein K, Woodhouse M, Bubb K, Dorrity MW, et al. (2018) Profiling of accessible chromatin regions across multiple plant species and cell types reveals common gene regulatory principles and new control modules. Plant Cell **30**: 15–36

Mao GH, Meng XZ, Liu YD, Zheng ZY, Chen ZX, Zhang SQ (2011) Phosphorylation of a WRKY transcription factor by two pathogen-responsive MAPKs drives phytoalexin biosynthesis in *Arabidopsis*. Plant Cell **23**: 1639–1653

Min HJ, Cui LH, Oh TR, Kim JH, Kim TW, Kim WT (2019) OsBZR1 turnover mediated by OsSK22-regulated U-box E3 ligase OsPUB24 in rice BR response. Plant J **99**: 426–438

Miura K, Jin JB, Lee J, Yoo CY, Stirm V, Miura T, Ashworth EN, Bressan RA, Yun DJ, Hasegawa PM. (2007) SIZ1-mediated sumoylation of ICE1 controls CBF3/DREB1A expression and freezing tolerance in *Arabidopsis*. Plant Cell **19**: 1403–1414.

Orosa B, Yates G, Verma V, Srivastava AK, Srivastava M, Campanaro A, De Vega D, Fernandes A, Zhang C, Lee J, et al. (2018) SUMO conjugation to the pattern recognition receptor FLS2 triggers intracellular signaling in plant innate immunity. Nat Commun **9**: 5185

Papdi C, Perez-Salamo I, Joseph MP, Giuntoli B, Bogre L, Koncz C, Szabados L (2015) The low oxygen, oxidative and osmotic stress responses synergistically act through the ethylene response factor VII genes RAP2.12, RAP2.2 and RAP2.3. Plant J **82**: 772–784

Qin F, Sakuma Y, Tran LP, Maruyama K, Kidokoro S, Fujita Y, Fujita M, Umezawa T, Sawano Y, Miyazono K, et al. (2008) *Arabidopsis* DREB2A-interacting proteins function as RING e3 ligases and negatively regulate plant drought stress-responsive gene expression. Plant Cell **20**: 1693–1707

Rhine MD, Stevens G, Shannon G, Wrather A, Sleper D (2010) Yield and nutritional responses to waterlogging of soybean cultivars. Irrigation Sci **28**: 135–142

Sadanandom A, Bailey M, Ewan R, Lee J, Nelis S (2012) The ubiquitin-proteasome system: central modifier of plant signalling. New Phytol **196**: 13–28

Sasidharan R, Voesenek LACJ (2015) Ethylene-mediated acclimations to flooding stress. Plant Physiol **169**: 3–12

Sasidharan R, Hartman S, Liu ZG, Martopawiro S, Sajeev N, vanVeen H, Yeung E, Voeseneka LACJ (2018) Signal dynamics and interactions during flooding stress. Plant Physiol **176**: 1106–1117

Spoel SH, Mou ZL, Tada Y, Spivey NW, Genschik P, Dong XNA (2009) Proteasome-mediated turnover of the transcription coactivator NPR1 plays dual roles in regulating plant immunity. Cell **137**: 860–872

Stone SL, Hauksdottir H, Troy A, Herschleb J, Kraft E, Callis J (2005) Functional analysis of the RING-type ubiquitin ligase family of *Arabidopsis*. Plant Physiol **137**:13–30

Tang H, Bi H, Liu B, Lou SL, Song Y, Tong SF, Chen NN, Jiang YZ, Liu JQ, Liu HH (2020) WRKY33 interacts with WRKY12 protein to up-regulate *RAP2.2* during submergence induced hypoxia response in *Arabidopsis thaliana*. New Phytol **229**: 106–125

Wang X, Ding YL, Li ZY, Shi YT, Wang JL, Hua J, Gong ZZ, Zhou JM, Yang SH (2019) PUB25 and PUB26 promote plant freezing tolerance by degrading the cold signaling negative regulator MYB15. Dev Cell **51**: 222–235

Xie LJ, Zhou Y, Chen QF, Xiao S (2020) New insights into the role of lipids in plant hypoxia responses. Prog Lipid Res **81**:101072

Yu LJ, Nie JN, Cao CY, Jin YK, Yan M, Wang FZ, Liu J, Xiao Y, Liang YH, Zhang WH (2010) Phosphatidic acid mediates salt stress response by regulation of MPK6 in *Arabidopsis thaliana*. New Phytol **188**: 762–773

Yuan LB, Dai YS, Xie LJ, Yu LJ, Zhou Y, Lai YX, Yang YC, Xu L, Chen QF, Xiao S (2017) Jasmonate regulates plant responses to postsubmergence reoxygenation through transcriptional activation of antioxidant synthesis. Plant Physiol **173**: 1864–1880

Zhan N, Wang C, Chen LC, Yang HJ, Feng J, Gong XQ, Ren B, Wu R, Mu JY, Li YS, et al. (2018) S-Nitrosylation targets GSNO reductase for selective autophagy during hypoxia responses in plants. Mol Cell **71**: 142–154

Zhang C, Xu YY, Guo SY, Zhu JY, Huan Q, Liu HH, Wang L, Luo GZ, Wang XJ, Chong K (2012) Dynamics of brassinosteroid response modulated by negative regulator LIC in rice. PLoS Genet **8**: e1002686

Zhang XR, Henriques R, Lin SS, Niu QW, Chua NH (2006) Agrobacterium-mediated transformation of *Arabidopsis thaliana* using the floral dip method. Nat Protocol **1**: 641–646

Zheng ZY, Abu Qamar S, Chen ZX, Mengiste T (2006) *Arabidopsis* WRKY33 transcription factor is required for resistance to necrotrophic fungal pathogens. Plant J **48**: 592–605

Zhou J, Wang J, Zheng ZY, Fan BF, Yu JQ, Chen ZX (2015) Characterization of the promoter and extended C-terminal domain of *Arabidopsis* WRKY33 and functional analysis of tomato WRKY33 homologues in plant stress responses. J Exp Bot **66**: 4567–4583

Zhu JY, Li YY, Cao DM, Yang HJ, Oh EY, Bi Y, Zhu SW, Wang ZY (2017) The f-box protein KIB1 mediates brassinosteroid-induced inactivation and degradation of GSK3-like kinases in *Arabidopsis*. Mol Cell **66**: 648–657